nature cell biology

α-catenin acts as a tumour suppressor in E-cadherin-negative basal-like breast cancer by inhibiting NF-κB signalling

Hai-long Piao[1], Yuan Yuan[2,3], Min Wang[1], Yutong Sun[4], Han Liang[2] and Li Ma[1,5,6]

Basal-like breast cancer is a highly aggressive tumour subtype associated with poor prognosis. Aberrant activation of NF-κB signalling is frequently found in triple-negative basal-like breast cancer cells, but the cause of this activation has remained elusive. Here we report that α-catenin functions as a tumour suppressor in E-cadherin-negative basal-like breast cancer cells by inhibiting NF-κB signalling. Mechanistically, α-catenin interacts with the IκBα protein, and stabilizes IκBα by inhibiting its ubiquitylation and its association with the proteasome. This stabilization in turn prevents nuclear localization of RelA and p50, leading to decreased expression of TNF-α, IL-8 and RelB. In human breast cancer, *CTNNA1* expression is specifically downregulated in the basal-like subtype, correlates with clinical outcome and inversely correlates with *TNF* and *RELB* expression. Taken together, these results uncover a previously undescribed mechanism by which the NF-κB pathway is activated in E-cadherin-negative basal-like breast cancer.

Breast cancer can be classified into three subtypes based on the membrane receptor status: oestrogen receptor (ER)+, HER2+ and triple-negative—defined by lack of expression of ER, progesterone receptor and HER2 (ref. 1). A molecular classification scheme, based on gene expression profiling, classifies breast cancer into the luminal A, luminal B, basal-like, normal-like and HER2+ subtypes[2,3]. Basal-like breast cancer is associated with a worse prognosis than are other subtypes[4,5]. Approximately 75% of triple-negative breast cancer cases are basal-like[6]. Patients with ER+ and HER2+ breast cancer are treated with tamoxifen and trastuzumab (or lapatinib), respectively[7,8], but so far there is no FDA (Food and Drug Administration)-approved targeted therapy for triple-negative breast cancer[4,5].

Cell–cell adherens junctions are intercellular junctions that are abundant in normal epithelia and reduced in cancers. The transmembrane core of adherens junctions is composed of E-cadherin, whose cytoplasmic domain interacts with β-catenin, which in turn binds to α-catenin[9]. α-catenin integrates adherens junctions with the actin cytoskeleton and promotes intercellular adhesion[9]. Alterations in adherens junction genes and their protein products are found in human cancer. The gene encoding E-cadherin, *CDH1*, is mutated in 7% of human breast cancers[10]. Loss of E-cadherin has been shown to induce breast cancer invasion and metastasis[11,12]. β-catenin, which links adherens junctions and the Wnt pathway, promotes both tumorigenesis and metastasis in multiple cancer types[13]. α-catenin is a putative tumour suppressor in myeloid leukaemia[14], glioblastoma[15] and skin cancer[16,17]. Loss of *CTNNA1* (the gene encoding α-catenin) causes global loss of cell adhesion in E-cadherin-expressing human breast carcinoma cells[18], which demonstrated the importance of α-catenin in maintaining the integrity of adherens junctions.

Hyperactivation of NF-κB signalling is frequently found in triple-negative basal-like breast cancer cells[19], but its cause is unclear. Genes regulated by the NF-κB pathway are implicated in various hallmarks of cancer, including proliferation, survival, cell death, invasion, angiogenesis and inflammation[20,21]. The five subunits of the NF-κB transcription factor family, RelA (p65), RelB, cRel, NF-κB1 (p50 and its precursor p105) and NF-κB2 (p52 and its precursor p100), form homodimers or heterodimers[22]. NF-κB signalling consists of canonical and non-canonical pathways[23]. In the canonical pathway, IκB, the inhibitor of NF-κB, sequesters the RelA–p50 heterodimer in the cytoplasm undernon-stimulated conditions. The key regulatory step

[1]Department of Experimental Radiation Oncology, The University of Texas MD Anderson Cancer Center, Houston, Texas 77030, USA. [2]Department of Bioinformatics and Computational Biology, The University of Texas MD Anderson Cancer Center, Houston, Texas 77030, USA. [3]Graduate Program in Structural and Computational Biology and Molecular Biophysics, Baylor College of Medicine, Houston, Texas 77030, USA. [4]Department of Molecular and Cellular Oncology, The University of Texas MD Anderson Cancer Center, Houston, Texas 77030, USA. [5]Cancer Biology Program, Graduate School of Biomedical Sciences, The University of Texas Health Science Center at Houston, Houston, Texas 77030, USA.

[6]Correspondence should be addressed to L.M. (e-mail: lma4@mdanderson.org)

Received 27 September 2013; accepted 19 December 2013; published online 9 February 2014; DOI: 10.1038/ncb2909

in this pathway involves ligand-induced activation of an IκB kinase (IKK) complex. The activated IKK complex phosphorylates IκB, which is then ubiquitylated and degraded. Subsequently, the RelA–p50 dimer enters the nucleus, where it regulates gene transcription[24]. In the non-canonical pathway, activated IKKα phosphorylates p100, the main inhibitor of RelB. The resulting processing of p100 then leads to RelB–p50 and RelB–p52 nuclear translocation and DNA binding[20]. Extensive efforts have been made to develop agents targeting the NF-κB pathway[20,25].

In the study reported herein, we investigated E-cadherin-independent functions of α-catenin and identified α-catenin as a tumour-suppressing protein in E-cadherin-negative basal-like breast cancer cells. Mechanistically, α-catenin inhibits tumorigenesis by interacting with IκBα, and the resulting stabilization of IκBα leads to cytoplasmic retention of RelA and downregulation of TNF-α, IL-8 and RelB. In human breast cancer, *CTNNA1* expression is specifically downregulated in the basal-like subtype and is negatively associated with NF-κB signalling.

RESULTS

α-catenin suppresses proliferation and colony formation of E-cadherin-negative basal-like breast cancer cells

α-catenin is a putative tumour suppressor in epithelial cancer cells that express E-cadherin, presumably owing to its essential role in maintaining the integrity of adherens junctions[18]. To investigate the role of α-catenin in E-cadherin-negative basal-like breast cancer cells, we first determined α-catenin protein levels in a panel of human mammary cell lines. Whereas immortalized human mammary epithelial (HMLE) cells and the MCF7 and T47D luminal breast cancer cells showed abundant α-catenin expression, this protein had moderate or negative expression in five of the six basal-like breast cancer cell lines tested: MDA-MB-231, SUM159, MDA-MB-436, MDA-MB-157 and MDA-MB-468. Only one basal-like cell line, BT549, exhibited α-catenin protein levels comparable to those in luminal-like cells (Fig. 1a). The MDA-MB-157 and MDA-MB-468 cell lines are α-catenin negative owing to a frameshift mutation in *CTNNA1* (ref. 26).

Next, we performed both loss-of-function and gain-of-function analyses of α-catenin in basal-like breast cancer cell lines (Fig. 1b,c). Two independent α-catenin short hairpin RNAs (shRNAs) both increased the proliferation of BT549 cells (Fig. 1d). In contrast, restoring α-catenin expression in MDA-MB-157 cells reduced their proliferation (Fig. 1d).

We also examined the effect of α-catenin loss on anchorage-independent growth and cell motility. In both BT549 and MDA-MB-231 cells, depletion of α-catenin significantly increased the cells' colony-forming ability in soft agar (Fig. 1e,f) and migratory ability (Fig. 1g). Knockdown of α-catenin in a luminal mammary cell line, MCF10A, also promoted oncogenic transformation and cell motility (Fig. 1h–j). Taken together, these results indicate that α-catenin may function as a tumour suppressor in both luminal and basal-like cells.

α-catenin inhibits NF-κB signalling in E-cadherin-negative basal-like breast cancer cells

The association with adherens junctions cannot explain the effect of α-catenin in E-cadherin-negative basal-like cells. To identify the signalling pathways regulated by α-catenin in basal-like cells, we performed a Human Cancer PathwayFinder quantitative PCR (qPCR) array analysis. Interestingly, all three most significantly downregulated genes in α-catenin-overexpressing MDA-MB-157 cells—*TNF*, *IL8* and *MMP1*—are NF-κB target genes[27–29] (Supplementary Table 1). To confirm that α-catenin downregulates NF-κB response genes, we performed qPCR analysis of two α-catenin-overexpressing E-cadherin-negative basal-like breast cancer cell lines, MDA-MB-157 and MDA-MB-436. Among several NF-κB target genes downregulated by α-catenin, the most markedly downregulated ones were *TNF* and *IL8* in MDA-MB-157 cells (Fig. 2a), which was consistent with the array results. Moreover, MDA-MB-157 and MDA-MB-436 cells with overexpression of α-catenin also exhibited a significant reduction in the levels of secreted TNF-α and IL-8 (Fig. 2b). In contrast, in the E-cadherin-positive, α-catenin-negative basal-like cell line MDA-MB-468, the levels of TNF-α, IL-8 and other components of the NF-κB pathway were either unaffected or upregulated on ectopic expression of α-catenin (Supplementary Fig. 1a–c). These findings indicate that α-catenin inhibits NF-κB signalling specifically in E-cadherin-negative basal-like breast cancer cells.

α-catenin stabilizes IκBα protein by inhibiting IκBα ubiquitylation

To further confirm that α-catenin inhibits NF-κB activity, we used a pNFκB luciferase reporter gene with specific NF-κB binding sites in the promoter region[30]. As anticipated, overexpression of α-catenin in MDA-MB-157 cells markedly suppressed the pNFκB luciferase activity and upregulated IκBα protein in the presence or absence of TNF-α stimulation, whereas neither RelA total protein level nor its phosphorylation was altered (Fig. 3a). Moreover, expression of α-catenin did not affect IKK phosphorylation in MDA-MB-157 cells (Supplementary Fig. 2), suggesting that the observed upregulation of IκBα by α-catenin was not due to the alteration in IKK activity.

In non-stimulated cells, RelA and NF-κB are sequestered in the cytoplasm by IκB inhibitory proteins, whereas TNF-α treatment induces degradation of IκB, leading to RelA and NF-κB nuclear translocation[20,24]. shRNA-mediated silencing of α-catenin decreased IκBα protein in TNF-α-treated BT549 cells (Fig. 3b), suggesting that α-catenin suppresses the response to TNF-α in these cells. In contrast, in luminal cell lines T47D and MCF10A, IκBα protein levels were not altered by knockdown of α-catenin, either with or without TNF-α treatment (Supplementary Fig. 3a–c).

In both MDA-MB-231 and MDA-MB-157 breast cancer cells, overexpression of α-catenin increased IκBα protein levels (Fig. 3c). In contrast to IκBα protein, *NFKBIA* messenger RNA (encoding IκBα) was downregulated in α-catenin-expressing cells (Fig. 3d), which suggested that α-catenin-mediated upregulation of IκBα might be due to increased protein stability instead of upregulation of its mRNA. We therefore examined IκBα protein levels in the presence of cycloheximide, an inhibitor of protein translation. As expected, overexpression of α-catenin in MDA-MB-157 cells significantly increased the stability of endogenous IκBα protein (Fig. 3e,f).

We next investigated whether α-catenin-mediated stabilization of IκBα involves the physical interaction of α-catenin with IκBα. Co-immunoprecipitation assays showed that overexpressed α-catenin

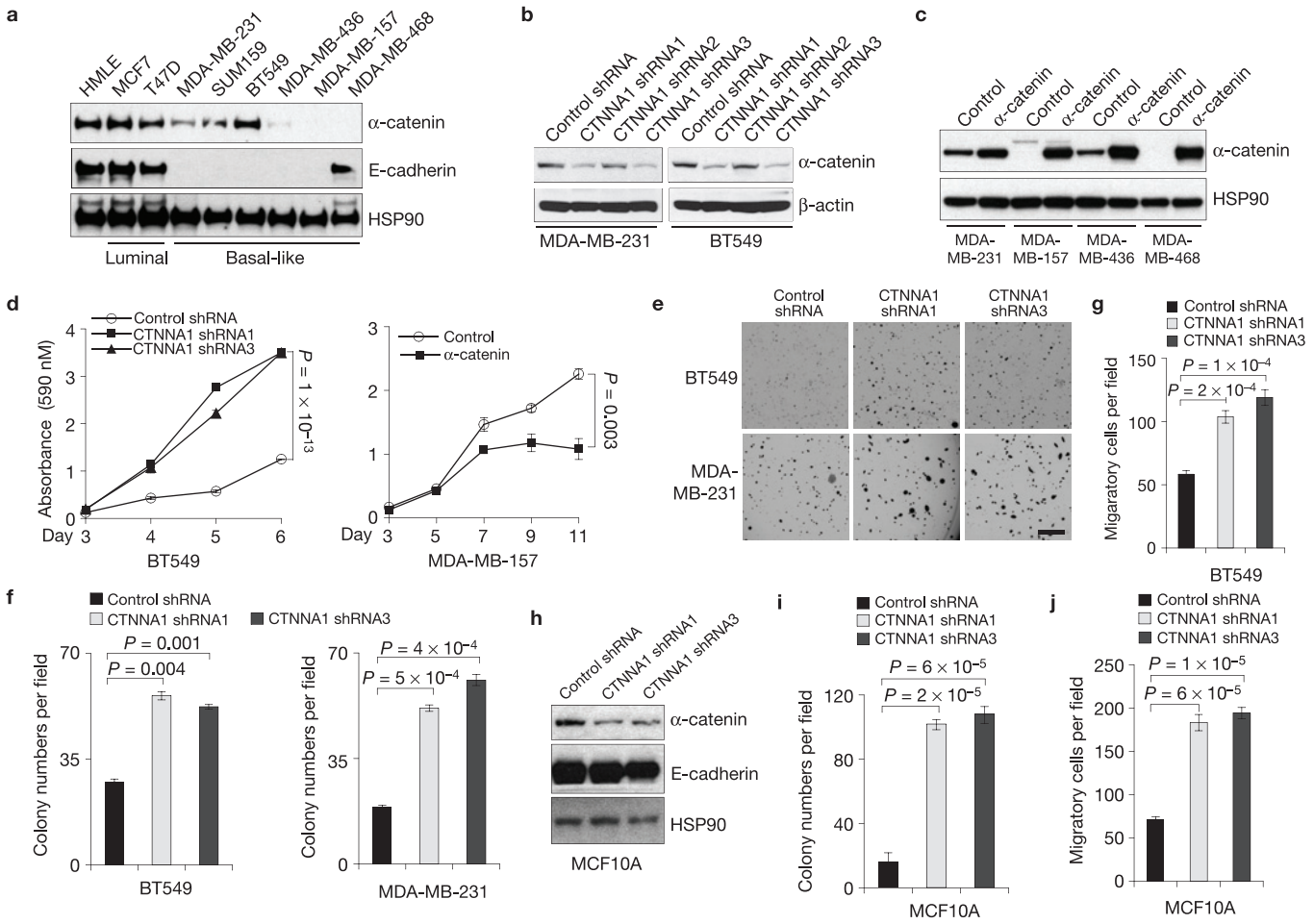

Figure 1 α-catenin inhibits proliferation and colony formation of basal-like breast cancer cells. (**a**) Immunoblotting of α-catenin, E-cadherin and HSP90 in HMLE, luminal and basal-like breast cancer cell lines. (**b**) Immunoblotting of α-catenin and β-actin in MDA-MB-231 and BT549 cells transduced with three independent α-catenin shRNAs. (**c**) Immunoblotting of α-catenin and HSP90 in α-catenin-transduced MDA-MB-231, MDA-MB-157, MDA-MB-436 and MDA-MB-468 cells. (**d**) Growth curves of BT549 cells with knockdown of α-catenin and MDA-MB-157 cells with ectopic expression of α-catenin. Control shRNA: the pGIPZ-GFP lentiviral vector with a scrambled sequence that does not target any mRNA. Control: the pLOC lentiviral vector with an RFP open reading frame. $n=4$ wells per group. (**e**,**f**) Representative images (**e**) and data quantification (**f**) of soft agar colony formation by BT549 and MDA-MB-231 cells transduced with two independent α-catenin shRNAs. Scale bar, 100 μm. $n=3$ wells per group. (**g**) Transwell migration assays of BT459 cells transduced with two independent α-catenin shRNAs. $n=3$ wells per group. (**h**) Immunoblotting of α-catenin, E-cadherin and HSP90 in MCF10A cells transduced with two independent α-catenin shRNAs. (**i**,**j**) Soft agar colony formation (**i**) and Transwell migration assays (**j**) of MCF10A cells transduced with two independent α-catenin shRNAs. $n=3$ wells per group. Data in **d**,**f**,**g**,**i**,**j** are the mean of biological replicates from a representative experiment, and error bars indicate s.e.m. Statistical significance was determined by a two-tailed, unpaired Student's *t*-test. The experiments were repeated three times. The source data can be found in Supplementary Table 4. Uncropped images of blots are shown in Supplementary Fig. 7.

could be detected in endogenous IκBα immunoprecipitates from MDA-MB-157 cells (Fig. 3g), and that endogenous IκBα was present in endogenous α-catenin immunoprecipitates from MDA-MB-231 and BT549 cells (Fig. 3h). This interaction did not require TNF-α stimulation (Fig. 3i). In contrast, α-catenin did not interact with IκBα in E-cadherin-positive luminal-like cell lines, T47D and MCF10A (Fig. 3j). In agreement with cytoplasmic sequestration of RelA by IκBα (refs 20,24), we observed existence of endogenous IκBα and RelA in endogenous α-catenin-containing protein complexes in both MDA-MB-231 and BT549 cells (Fig. 3h). β-catenin was also detectable in α-catenin immunoprecipitates (Fig. 3h). However, knockdown or overexpression of α-catenin did not affect β-catenin protein level, localization or activity in basal-like breast cancer cells (Supplementary Fig. 4). It has been reported that α-catenin contains three vinculin homology (VH) domains[31]: VH1, VH2 and VH3 (Fig. 3k). Although all three VH domains exhibited association with IκBα, the VH1 fragment showed the strongest interaction (Fig. 3k).

To address how α-catenin increases IκBα protein stability, we examined ubiquitylation of IκBα. Expression of α-catenin markedly reduced the polyubiquitylation level of IκBα, and this effect was abrogated when wild-type ubiquitin was substituted with a K48R mutant, but not a K63R mutant (Fig. 3l), suggesting that α-catenin inhibits Lys-48-linked ubiquitylation, which is known to be involved in protein degradation[32]. Moreover, the interaction of IκBα with the proteasome α4 subunit was abolished on α-catenin overexpression (Fig. 3m). We therefore conclude that α-catenin interacts with IκBα, inhibits IκBα polyubiquitylation, abrogates IκBα interaction with the proteasome and, as a result, stabilizes IκBα.

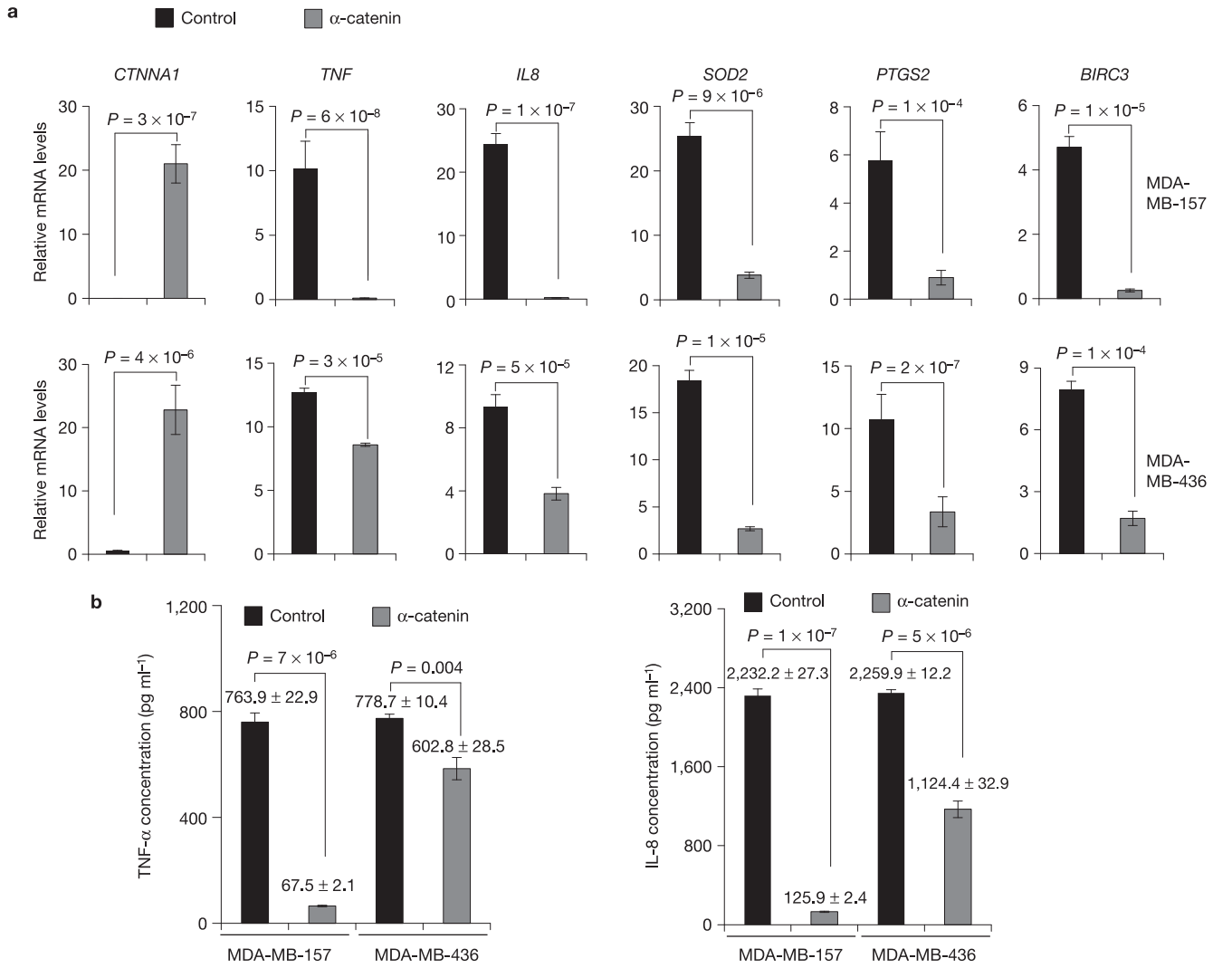

Figure 2 α-catenin inhibits NF-κB signalling in basal-like breast cancer cells. (**a**) qPCR of NF-κB response genes in α-catenin-transduced MDA-MB-157 and MDA-MB-436 cells. $n = 3$ samples per group. (**b**) Enzyme-linked immunosorbent assay of TNF-α and IL-8 secreted by α-catenin-transduced MDA-MB-157 and MDA-MB-436 cells. $n = 3$ wells per group. Data in **a**,**b** are the mean of biological replicates from a representative experiment, and error bars indicate s.e.m. Statistical significance was determined by a two-tailed, unpaired Student's *t*-test. The experiments were repeated three times. The source data can be found in Supplementary Table 4.

α-catenin inhibits RelA–p50 nuclear localization and downregulates RelB

Activation of the canonical NF-κB pathway leads to nuclear translocation of the RelA–p50 dimer, which functions as a transcriptional activator[20,24]. Compared with control shRNA-infected BT549 cells, two independent α-catenin shRNAs both induced nuclear translocation of RelA in response to TNF-α treatment (Fig. 4a), consistent with the effect on IκBα (Fig. 3b). Moreover, compared with mock-infected MDA-MB-157 cells, α-catenin-overexpressing MDA-MB-157 cells had increased cytoplasmic RelA and reduced nuclear RelA and p50, as gauged by fractionation assays (Fig. 4b).

Besides activating the transcription of *TNF* and *IL8*, RelA can also induce *RELB* expression through direct binding of the *RELB* promoter[33]. We therefore reasoned that α-catenin-mediated cytoplasmic retention of RelA may lead to reduced binding of the *RELB* promoter by RelA. To investigate this possibility, we performed chromatin immunoprecipitation (ChIP) assays of α-catenin-overexpressing MDA-MB-157 cells, followed by qPCR of the conserved *RELB* promoter region encompassing two consensus RelA-binding motifs (Fig. 4c). Chromatin immunoprecipitates with the RelA antibody were enriched for the *RELB* promoter region compared with those precipitated with the IgG control, confirming that this region does contain the RelA-binding site (Fig. 4d). Expression of α-catenin resulted in an approximately 50% reduction in binding of the *RELB* promoter by RelA (Fig. 4d). In agreement with these findings, overexpression of α-catenin in MDA-MB-157 and MDA-MB-436 cells downregulated both mRNA (Fig. 4e) and protein (Fig. 4b,f) levels of RelB. These findings confirm that α-catenin suppresses RelA–p50 nuclear localization, leading to inhibition of *RELB* transcription.

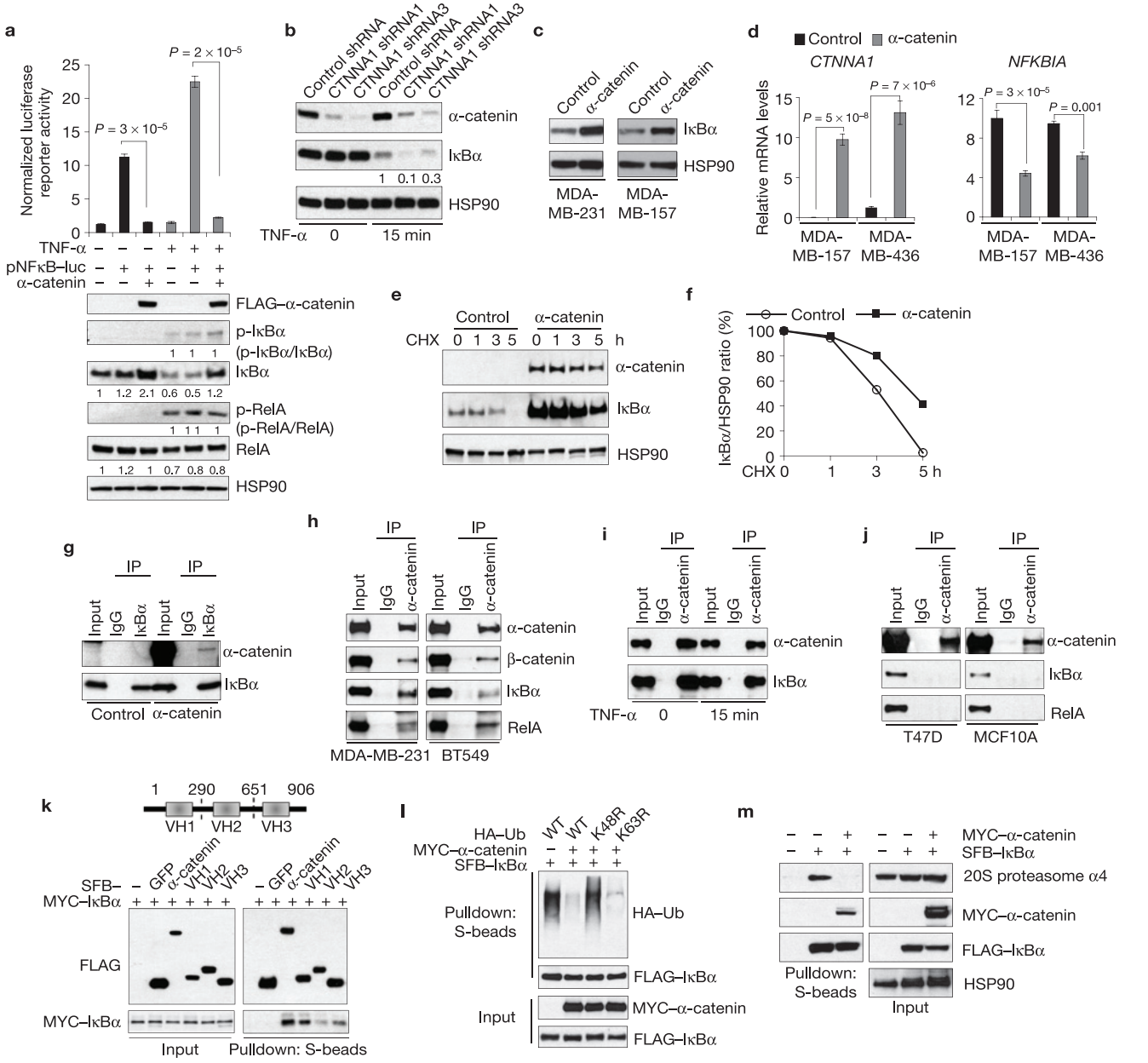

Figure 3 α-catenin stabilizes IκBα protein by inhibiting IκBα ubiquitylation and abrogating IκBα interaction with the proteasome. (**a**) Upper panel: luciferase assays of NF-κB activity in MDA-MB-157 cells transfected with a pNF-κB luciferase reporter alone or in combination with FLAG–α-catenin, with or without TNF-α treatment. Lower panel: immunoblotting of FLAG, p-IκBα, IκBα, p-RelA, RelA and HSP90. $n = 3$ wells per group. (**b**) Immunoblotting of α-catenin, IκBα and HSP90 in α-catenin shRNA-transduced BT549 cells, with or without TNF-α treatment. (**c**) Immunoblotting of IκBα and HSP90 in α-catenin-transduced MDA-MB-231 and MDA-MB-157 cells. (**d**) qPCR of *CTNNA1* and *NFKBIA* in α-catenin-transduced MDA-MB-157 and MDA-MB-436 cells. $n = 3$ samples per group. (**e**) α-catenin-transduced MDA-MB-157 cells were treated with 100 μg ml^{-1} of cycloheximide (CHX), collected at different time points and immunoblotted with antibodies against α-catenin, IκBα and HSP90. (**f**) Quantification of IκBα protein levels in **e**. (**g**) α-catenin was immunoprecipitated from α-catenin-transduced MDA-MB-157 cells and immunoblotted with antibodies against α-catenin and IκBα. (**h**) α-catenin was immunoprecipitated from MDA-MB-231 and BT549 cells and immunoblotted with antibodies against α-catenin, β-catenin, IκBα and RelA. (**i**) α-catenin was immunoprecipitated from untreated or TNF-α-treated BT549 cells and immunoblotted with antibodies against α-catenin and IκBα. (**j**) α-catenin was immunoprecipitated from T47D or MCF10A cells and immunoblotted with antibodies against α-catenin, IκBα and RelA. (**k**) Upper panel: schematic representation of three vinculin domains of α-catenin. Lower panel: HEK293T cells were co-transfected with MYC–IκBα and SFB-tagged full-length α-catenin or fragment VH1, VH2 or VH3. α-catenin and the three fragments were purified with S-protein beads and immunoblotted with antibodies against FLAG and MYC. (**l**) HA-tagged wild-type ubiquitin (Ub) or the K48R or K63R mutant was co-transfected with MYC–α-catenin and SFB–IκBα into HEK293T cells. Cells were treated with 10 μM MG132 and 20 ng ml^{-1} of TNF-α for 30 min. IκBα was purified with S-protein beads and immunoblotted with antibodies against HA and FLAG. (**m**) HEK293T cells were co-transfected with MYC–α-catenin and SFB–IκBα, and then treated with 10 μM MG132 and 20 ng ml^{-1} of TNF-α for 30 min. IκBα was purified with S-protein beads and immunoblotted with antibodies against the 20S proteasome subunit α4, MYC and FLAG. Data in **a**,**d** are the mean of biological replicates from a representative experiment, and error bars indicate s.e.m. Statistical significance was determined by a two-tailed, unpaired Student's *t*-test. The experiments were repeated three times. The source data can be found in Supplementary Table 4. Uncropped images of blots are shown in Supplementary Fig. 7.

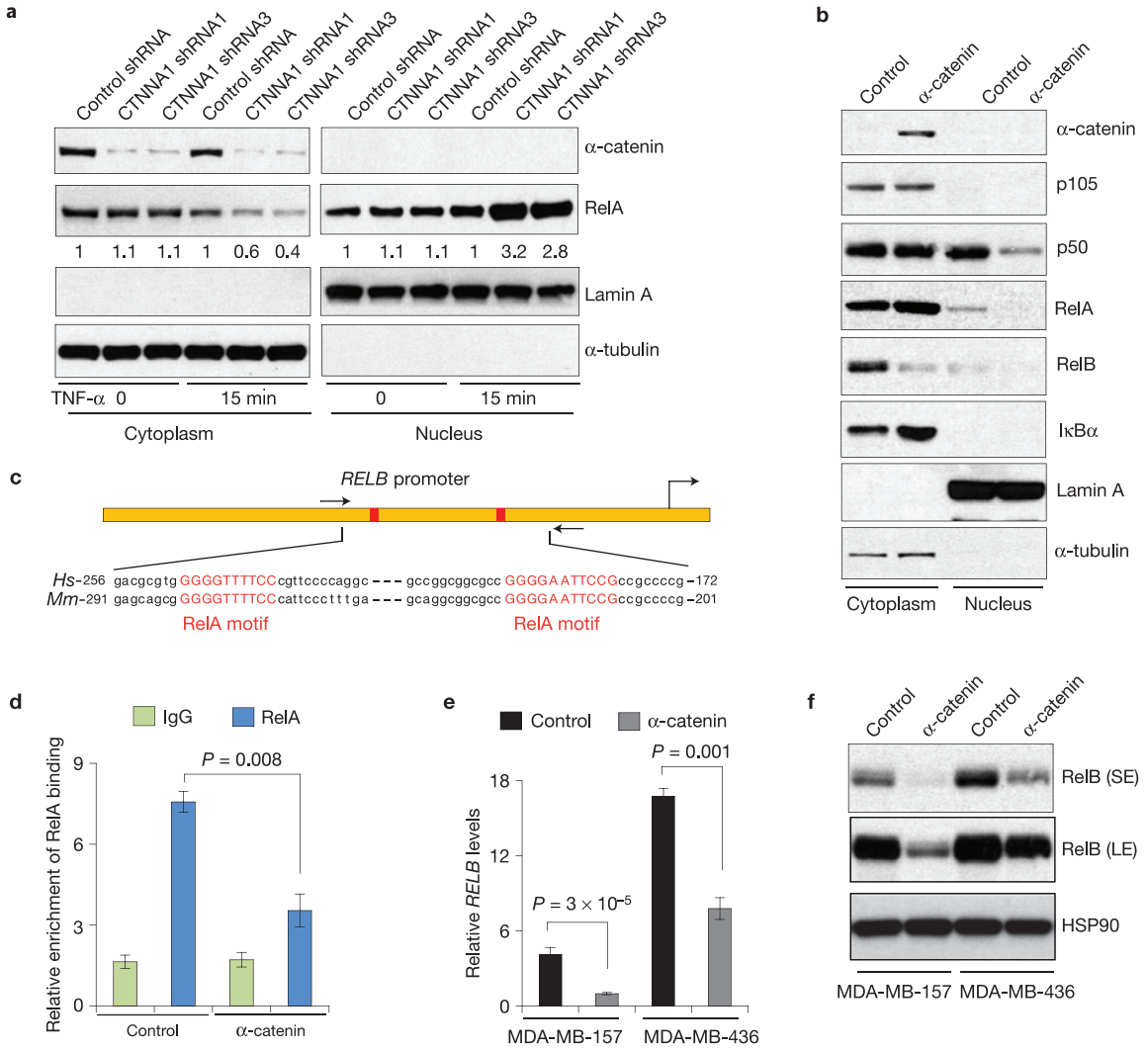

Figure 4 α-catenin inhibits RelA–p50 nuclear localization and downregulates RelB. (**a**) Immunoblotting of α-catenin and RelA in cytoplasmic and nuclear fractions of BT549 cells transduced with two independent α-catenin shRNAs, with or without TNF-α treatment. (**b**) Immunoblotting of α-catenin, p105, p50, RelA, RelB and IκBα in cytoplasmic and nuclear fractions of α-catenin-transduced MDA-MB-157 cells. α-tubulin and lamin A were used as cytoplasmic and nuclear markers, respectively, in **a**,**b**. (**c**) Schematic representation of the *RELB* promoter containing two RelA-binding sites (red). The two arrows indicate the primers used for ChIP-qPCR. *Hs*, *Homo sapiens*; *Mm*, *Mus musculus*. (**d**) ChIP-qPCR analysis of RelA binding to the *RELB* promoter in α-catenin-transduced MDA-MB-157 cells. qPCR was performed with primers specific to the RelA-binding motifs. Data were normalized to the input. $n = 3$ samples per group. (**e**) qPCR of *RELB* in α-catenin-transduced MDA-MB-157 and MDA-MB-436 cells. $n = 3$ samples per group. (**f**) Immunoblotting of RelB and HSP90 in α-catenin-transduced MDA-MB-157 and MDA-MB-436 cells. SE, short exposure; LE, long exposure. Data in **d**,**e** are the mean of biological replicates from a representative experiment, and error bars indicate s.e.m. Statistical significance was determined by a two-tailed, unpaired Student's *t*-test. The experiments were repeated three times. The source data can be found in Supplementary Table 4. Uncropped images of blots are shown in Supplementary Fig. 7.

α-catenin functions as a tumour suppressor in basal-like breast cancer cells by inhibiting NF-κB signalling

To determine whether NF-κB mediates the growth-promoting effect of α-catenin shRNA, we expressed two independent RelA shRNAs in α-catenin-depleted MDA-MB-231 and BT549 cells (Fig. 5a). In both cell lines, knockdown of RelA reversed the effect of α-catenin shRNA on promoting anchorage-independent growth (Fig. 5b).

To explore the function of α-catenin in basal-like breast cancer cells *in vivo*, we subcutaneously implanted α-catenin-depleted BT549 and MDA-MB-231 cells with or without expression of RelA shRNA into nude mice. Hosts of α-catenin shRNA-expressing cancer cells had larger tumour volumes throughout the experiment than mice implanted with control shRNA-infected cells (Fig. 5c). At 5 weeks after tumour cell implantation, we observed a 2.8-fold increase and a 2.2-fold increase in the weight of the tumours formed by α-catenin-depleted MDA-MB-231 and BT549 cells, respectively (Fig. 5d,e). Notably, the tumour growth of α-catenin-depleted cells that also expressed RelA shRNA was similar to the tumour growth of control shRNA-infected cells (Fig. 5c–e). Compared with the tumours formed by control MDA-MB-231 cells or MDA-MB-231 cells with simultaneous knockdown of α-catenin and RelA, α-catenin-depleted MDA-MB-231 tumours exhibited upregulation of TNF-α (Fig. 5f) and

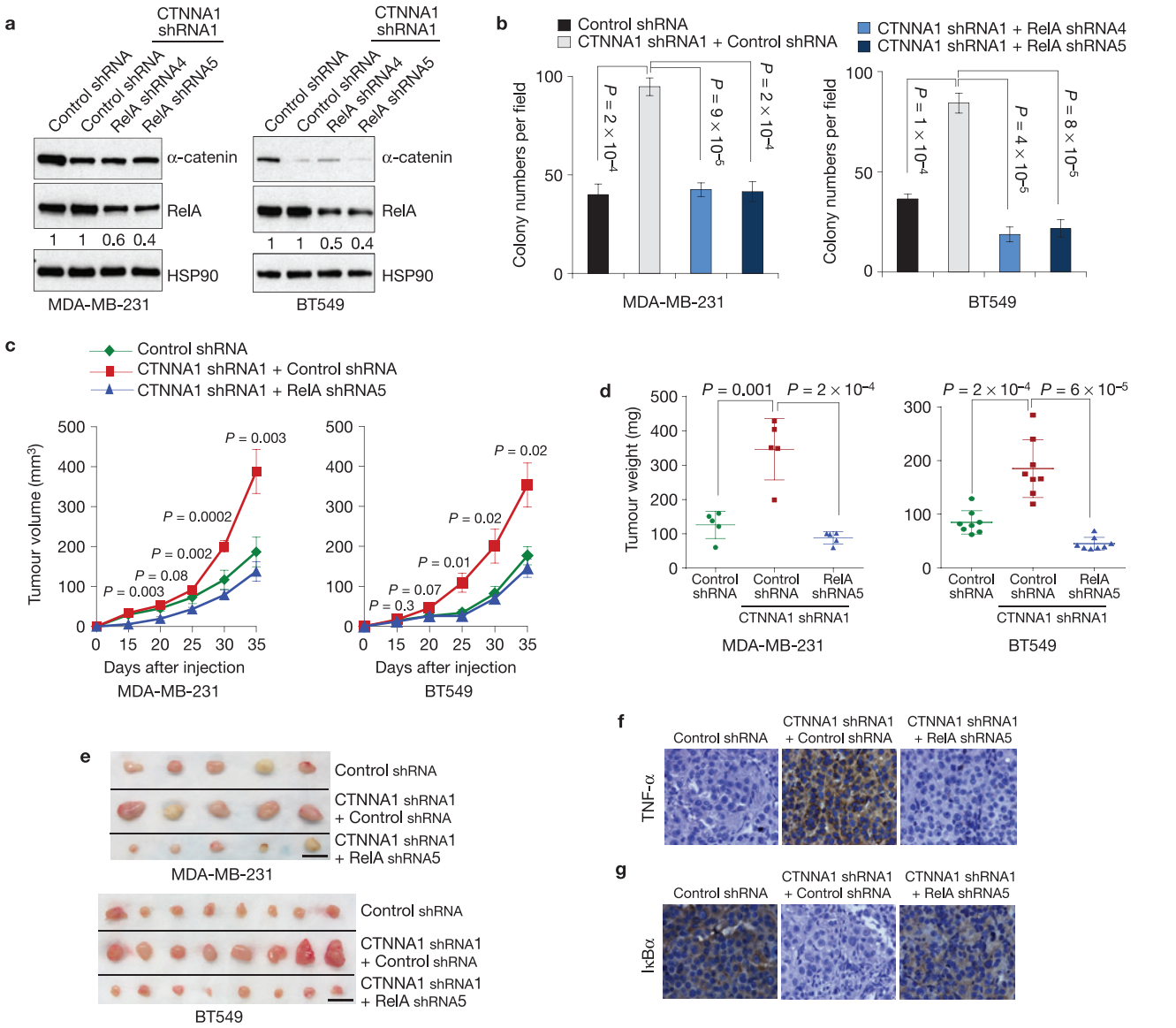

Figure 5 Loss of α-catenin promotes tumour growth in basal-like breast cancer cells by activating NF-κB signalling. (**a**) Immunoblotting of α-catenin, RelA and HSP90 in MDA-MB-231 and BT549 cells transduced with α-catenin shRNA alone or in combination with RelA shRNA. (**b**) Soft agar colony formation by MDA-MB-231 and BT549 cells transduced with α-catenin shRNA alone or in combination with RelA shRNA. $n=4$ wells per group. (**c**) Tumour growth by subcutaneously implanted MDA-MB-231 (3×10^6 cells injected) or BT549 (4×10^6 cells injected) cells infected with α-catenin shRNA alone or in combination with RelA shRNA. *P* values correspond to comparisons between α-catenin shRNA alone and α-catenin shRNA in combination with RelA shRNA. (**d**,**e**) Tumour weight (**d**) and tumour images (**e**) 5 weeks after mice were injected subcutaneously with MDA-MB-231 or BT549 cells transduced with α-catenin shRNA alone or in combination with RelA shRNA. Scale bar, 1 cm. $n=5$ (for MDA-MB-231 cells) or 8 (for BT549 cells) mice per group in **c**,**d**. (**f**,**g**) TNF-α (**f**) and human-specific IκBα (**g**) immunohistochemical staining of subcutaneous tumours formed by MDA-MB-231 cells transduced with α-catenin shRNA alone or in combination with RelA shRNA, at 5 weeks after implantation. Scale bar, 50 μm. Data in **b**–**d** are the mean of biological replicates from a representative experiment, and error bars indicate s.e.m. Statistical significance was determined by a two-tailed, unpaired Student's *t*-test. The experiments were repeated three times. The source data can be found in Supplementary Table 4. Uncropped images of blots are shown in Supplementary Fig. 7.

downregulation of IκBα (Fig. 5g), suggesting that loss of α-catenin can lead to activation of NF-κB signalling *in vivo*.

To further confirm that α-catenin suppresses tumorigenesis by inhibiting NF-κB signalling, we used two independent shRNAs to silence IκBα in α-catenin-overexpressing MDA-MB-157 cells. Knockdown of IκBα rescued RelB expression (Fig. 6a), *in vitro* cell proliferation (Fig. 6b,c) and colony formation (Fig. 6d,e). We then implanted these cells subcutaneously into mice. Notably, mice implanted with either the control MDA-MB-157 cells or MDA-MB-157 cells with simultaneous α-catenin overexpression and IκBα knockdown showed similar tumour growth rates, whereas mice bearing α-catenin-overexpressing MDA-MB-157 cells showed markedly inhibited tumorigenesis (Fig. 6f–h). Taken together, these results suggest that stabilization of IκBα mediates, at least in part, the tumour-suppressing effect of α-catenin in E-cadherin-negative basal-like breast cancer cells.

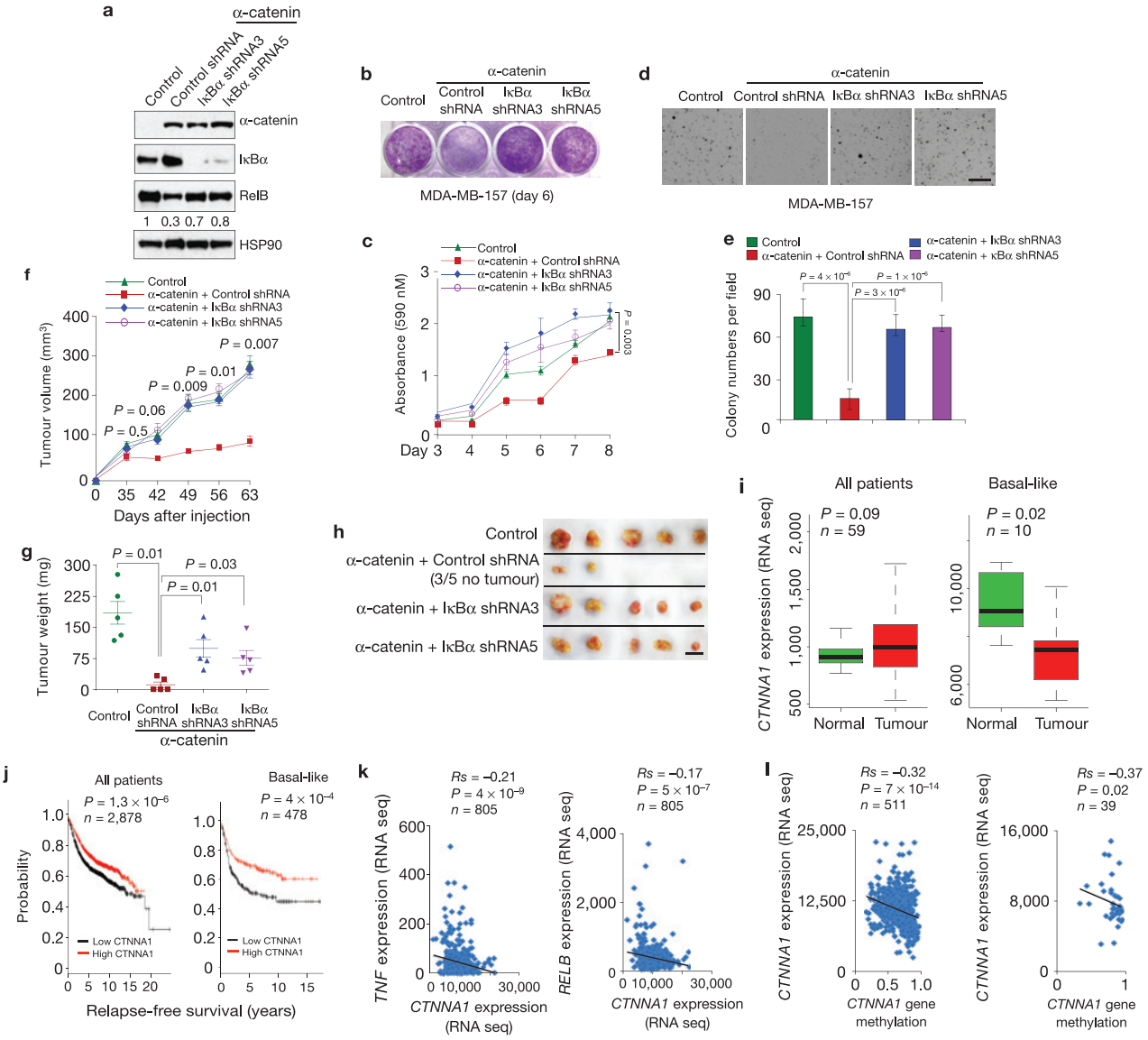

Figure 6 α-catenin inhibits tumorigenesis and is downregulated in human basal-like breast cancer. (**a**) Immunoblotting of α-catenin, IκBα, RelB and HSP90 in MDA-MB-157 cells transduced with α-catenin alone or in combination with IκBα shRNA. (**b**,**c**) Images (**b**) and quantification (**c**) of growth curves of cells described in **a**. $n=3$ wells per group. (**d**,**e**) Images (**d**) and quantification (**e**) of soft agar colony formation by cells described in **a**. Scale bar, 100 μm. $n=5$ wells per group. (**f**) Tumour growth by 3×10^6 subcutaneously injected cells described in **a**. *P* values correspond to comparisons between α-catenin alone and α-catenin in combination with IκBα shRNA (IκBα shRNA3) in **c**,**f**. (**g**,**h**) Tumour weight (**g**) and tumour images (**h**) of the mice described in **f**. Scale bar, 1 cm. $n=5$ mice per group in **f**,**g**. (**i**) Box plots comparing *CTNNA1* expression in normal breast tissues and in total ($n=59$) and basal-like ($n=10$) breast tumours. Statistical significance was determined by the Wilcoxon test. The boxes show the median and the interquartile range. The whiskers show the minimum and maximum. (**j**) Kaplan–Meier curves of relapse-free survival times of total breast cancer patients ($n=2,878$) and patients with basal-like breast cancer ($n=478$), stratified by *CTNNA1* expression levels. Data were obtained from http://kmplot.com/analysis/ (ref. 34). Statistical significance was determined by the log-rank test. (**k**) Scatter plots showing the inverse correlation of *CTNNA1* with *TNF* (left panel) or *RELB* (right panel) expression in human breast tumours ($n=805$). (**l**) Scatter plots showing the inverse correlation between methylation of the *CTNNA1* gene and *CTNNA1* expression in total (left panel, $n=511$) and basal-like (right panel, $n=39$) breast tumours. Statistical significance in **k**,**l** was determined by the Spearman rank correlation test. *Rs*, Spearman rank correlation coefficient. Data in **c**,**e**–**g** are the mean of biological replicates from a representative experiment, and error bars indicate s.e.m. Statistical significance was determined by a two-tailed, unpaired Student's *t*-test. The experiments were repeated three times. The source data can be found in Supplementary Table 4. Uncropped images of blots are shown in Supplementary Fig. 7.

α-catenin expression is downregulated in human basal-like breast tumours and negatively correlates with the activity of the NF-κB pathway

To investigate the relevance of our findings to human breast cancer, we analysed gene expression data from The Cancer Genome Atlas[10] (TCGA). We found that *CTNNA1* expression was significantly downregulated in the basal-like subtype of breast cancer compared with normal breast tissues, whereas other breast cancer subtypes exhibited either upregulation of *CTNNA1* or no significant difference (Fig. 6i and Supplementary Fig. 5a). We also evaluated the prognostic

value of *CTNNA1* in a microarray data set of breast tumours from 2,878 patients[34]. Of 478 patients with basal-like breast cancer, those with low levels of *CTNNA1* (the median value was used as the cutoff for low and high expression) had much shorter relapse-free survival ($P = 4 \times 10^{-4}$) than did patients with high levels of *CTNNA1*, whereas the difference in patients with other subtypes of breast cancer was either not significant or less significant (Fig. 6j and Supplementary Fig. 5b).

Next, we investigated whether *CTNNA1* expression is negatively associated with the activity of NF-κB signalling. Both RNA-sequencing and microarray data from TCGA (ref. 10) revealed a significant inverse correlation of *CTNNA1* with *TNF* and *RELB* expression levels in human breast tumours (Fig. 6k and Supplementary Fig. 5c).

We examined how α-catenin expression is downregulated or lost in breast cancer. Although *CTNNA1* gene deletion was found in tumours from one basal-like breast cancer patient[35], analysis of breast cancer data from TCGA (ref. 10) revealed that deletion (1 of 482 patients) or mutation (4 of 482 patients) of *CTNNA1* was rare. On the other hand, we observed a significant inverse correlation between *CTNNA1* mRNA level and *CTNNA1* gene methylation in both total and basal-like breast tumours (Fig. 6l), which indicated that *CTNNA1* gene hypermethylation, but not genetic alteration, is likely to be a main cause of α-catenin downregulation or loss in human breast cancer.

DISCUSSION

We conclude that α-catenin acts as a tumour-suppressing protein in multiple cancer types and subtypes, but the mechanism of action varies depending on the tissue type. In epidermal cells, α-catenin inhibits tumorigenesis by inducing phosphorylation, cytoplasmic retention and functional inactivation of the oncoprotein YAP (refs 16,17; Supplementary Fig. 6a, left panel). However, we did not observe this effect on YAP phosphorylation in the basal-like breast cancer cell lines MDA-MB-157 and MDA-MB-436 (Supplementary Fig. 6b). Moreover, α-catenin is a structural link between the E-cadherin–catenin complex and the actin cytoskeleton and is involved in epithelial tumour suppression[9,18] (Supplementary Fig. 6a, left panel), but this mechanism is irrelevant in basal-like cells that have lost E-cadherin expression. In the present study, we identified α-catenin as a tumour-suppressing protein in E-cadherin-negative basal-like breast cancer cells and found that α-catenin inhibits NF-κB signalling by stabilizing IκBα and sequestering RelA–p50 in the cytoplasm (Supplementary Fig. 6a, right panel). In contrast, α-catenin does not inhibit the NF-κB pathway in luminal cells or E-cadherin-positive basal-like cells, indicating that when localized at the E-cadherin–catenin complex, α-catenin may not be capable of regulating IκBα ubiquitylation and RelA–p50 localization, at least in mammary cells. It should be noted that ref. 36 demonstrated deregulation of NF-κB signalling components in α-catenin-deficient mouse skin cells, but the functional relevance and the mechanistic link have not been determined in the skin.

The effect of α-catenin shRNA on IκBα stability (Fig. 3b) and RelA nuclear translocation (Fig. 4a) was observed only on stimulation with TNF-α. Similarly, it has been shown that deletion of either IKKα or IKKβ stabilized IκBα protein in TNF-α-treated mouse embryonic fibroblast cells, but had no effect on IκBα stability in non-stimulated mouse embryonic fibroblasts[37,38]. This loss-of-function effect of α-catenin is biologically relevant, because cancer cells within a tumour are usually exposed to TNF-α secreted by infiltrated macrophages or by tumour cells themselves.

The NF-κB pathway can be activated by a variety of stimuli[21]. Activated NF-κB regulates approximately 200 target genes encoding cytokines, chemokines, growth factors and transcription factors[21,39,40]. Aberrant activation of NF-κB signalling is associated with various human cancers including breast cancer[41]. Although HER2 can trigger NF-κB activation through the PI(3)K/AKT pathway[42], the cause of the elevated NF-κB activity frequently observed in triple-negative basal-like breast cancer cells[19] remains elusive. Our findings identify loss of α-catenin as a mechanism by which the NF-κB pathway is activated in the basal-like subtype of breast cancer. This is highly relevant in human tumours, as α-catenin is specifically downregulated in human basal-like breast cancer, correlates with recurrence-free survival and negatively correlates with the activity of NF-κB signalling. Targeting the NF-κB pathway may provide therapeutic benefits to patients with basal-like, triple-negative breast cancer. □

METHODS

Methods and any associated references are available in the online version of the paper.

Note: Supplementary Information is available in the online version of the paper

ACKNOWLEDGEMENTS

We thank S. Ethier (Medical University of South Carolina, USA) for the SUM159 cell line; J. Chen (The University of Texas MD Anderson Cancer Center, USA) for plasmids; the shRNA and ORFeome Core and the Histology Core at The University of Texas MD Anderson Cancer Center for technical assistance; J. Zhang and J. Chen for assistance with graphics; J. M. Rosen, X. Lin, W. Wang and members of the Ma laboratory for discussion; and H-l. Piao, C. Chu and A. Gelmis for editing the manuscript. This work is supported by US National Institutes of Health grants R00CA138572 (to L.M.) and R01CA166051 (to L.M.) and a Cancer Prevention and Research Institute of Texas Scholar Award R1004 (to L.M.).

AUTHOR CONTRIBUTIONS

L.M. conceived and supervised the project. H-l.P. designed, performed and analysed most of the experiments. Y.Y. and H.L. performed computational data analysis. M.W. performed immunohistochemical staining and provided animal care. Y.S. maintained shRNA and ORF clones and provided significant intellectual input. H-l.P. and L.M. wrote the manuscript with input from all other authors.

COMPETING FINANCIAL INTERESTS

The authors declare no competing financial interests.

Published online at www.nature.com/doifinder/10.1038/ncb2909
Reprints and permissions information is available online at www.nature.com/reprints

1. Di Cosimo, S. & Baselga, J. Management of breast cancer with targeted agents: importance of heterogeneity. [corrected]. *Nat. Rev. Clin. Oncol.* **7,** 139–147 (2010).
2. Perou, C. M. *et al.* Molecular portraits of human breast tumours. *Nature* **406,** 747–752 (2000).
3. Sorlie, T. *et al.* Repeated observation of breast tumor subtypes in independent gene expression data sets. *Proc. Natl Acad. Sci. USA* **100,** 8418–8423 (2003).
4. Prat, A. & Perou, C. M. Deconstructing the molecular portraits of breast cancer. *Mol. Oncol.* **5,** 5–23 (2011).
5. Rakha, E. A., El-Sayed, M. E., Reis-Filho, J. & Ellis, I. O. Patho-biological aspects of basal-like breast cancer. *Breast Cancer Res. Treat.* **113,** 411–422 (2009).
6. Perou, C. M. Molecular stratification of triple-negative breast cancers. *Oncologist* **16** (Suppl 1), 61–70 (2011).
7. Osborne, C. K. Tamoxifen in the treatment of breast cancer. *New Engl. J. Med.* **339,** 1609–1618 (1998).
8. Slamon, D. J. *et al.* Studies of the HER-2/neu proto-oncogene in human breast and ovarian cancer. *Science* **244,** 707–712 (1989).
9. Kobielak, A. & Fuchs, E. α-catenin: at the junction of intercellular adhesion and actin dynamics. *Nat. Rev. Mol. Cell Biol.* **5,** 614–625 (2004).

10. The Cancer Genome Atlas Network, Comprehensive molecular portraits of human breast tumours. *Nature* **490,** 61–70 (2012).
11. Onder, T. T. *et al.* Loss of E-cadherin promotes metastasis via multiple downstream transcriptional pathways. *Cancer Res.* **68,** 3645–3654 (2008).
12. Derksen, P. W. *et al.* Somatic inactivation of E-cadherin and p53 in mice leads to metastatic lobular mammary carcinoma through induction of anoikis resistance and angiogenesis. *Cancer Cell* **10,** 437–449 (2006).
13. Fodde, R. & Brabletz, T. Wnt/β-catenin signaling in cancer stemness and malignant behavior. *Curr. Opin. Cell Biol.* **19,** 150–158 (2007).
14. Liu, T. X. *et al.* Chromosome 5q deletion and epigenetic suppression of the gene encoding α-catenin (CTNNA1) in myeloid cell transformation. *Nat. Med.* **13,** 78–83 (2007).
15. Ji, H., Wang, J., Fang, B., Fang, X. & Lu, Z. α-Catenin inhibits glioma cell migration, invasion, and proliferation by suppression of β-catenin transactivation. *J. Neurooncol.* **103,** 445–451 (2011).
16. Schlegelmilch, K. *et al.* Yap1 acts downstream of α-catenin to control epidermal proliferation. *Cell* **144,** 782–795 (2011).
17. Silvis, M. R. *et al.* α-catenin is a tumor suppressor that controls cell accumulation by regulating the localization and activity of the transcriptional coactivator Yap1. *Sci. Signal.* **4,** ra33 (2011).
18. Bajpai, S., Feng, Y., Krishnamurthy, R., Longmore, G. D. & Wirtz, D. Loss of α-catenin decreases the strength of single E-cadherin bonds between human cancer cells. *J. Biol. Chem.* **284,** 18252–18259 (2009).
19. Yamaguchi, N. *et al.* Constitutive activation of nuclear factor-κB is preferentially involved in the proliferation of basal-like subtype breast cancer cell lines. *Cancer Sci.* **100,** 1668–1674 (2009).
20. Baud, V. & Karin, M. Is NF-κB a good target for cancer therapy? Hopes and pitfalls. *Nat. Rev. Drug Discov.* **8,** 33–40 (2009).
21. Pahl, H. L. Activators and target genes of Rel/NF-κB transcription factors. *Oncogene* **18,** 6853–6866 (1999).
22. Hayden, M. S. & Ghosh, S. Signaling to NF-κB. *Genes Dev.* **18,** 2195–2224 (2004).
23. Baltimore, D. Discovering NF-κB. *Cold Spring Harb. Perspect. Biol.* **1,** a000026 (2009).
24. Karin, M., Yamamoto, Y. & Wang, Q. M. The IKK NF-κB system: a treasure trove for drug development. *Nat. Rev. Drug Discov.* **3,** 17–26 (2004).
25. Basseres, D. S. & Baldwin, A. S. Nuclear factor-κB and inhibitor of κB kinase pathways in oncogenic initiation and progression. *Oncogene* **25,** 6817–6830 (2006).
26. Hollestelle, A. *et al.* Four human breast cancer cell lines with biallelic inactivating α-catenin gene mutations. *Breast Cancer Res. Treat.* **122,** 125–133 (2010).
27. Collart, M. A., Baeuerle, P. & Vassalli, P. Regulation of tumor necrosis factor α transcription in macrophages: involvement of four κB-like motifs and of constitutive and inducible forms of NF-κB. *Mol. Cell Biol.* **10,** 1498–1506 (1990).
28. Kunsch, C. & Rosen, C. A. NF-κB subunit-specific regulation of the interleukin-8 promoter. *Mol. Cell Biol.* **13,** 6137–6146 (1993).
29. Vincenti, M. P., Coon, C. I. & Brinckerhoff, C. E. Nuclear factor κB/p50 activates an element in the distal matrix metalloproteinase 1 promoter in interleukin-1β-stimulated synovial fibroblasts. *Arthritis Rheum.* **41,** 1987–1994 (1998).
30. Matluk, N., Rochira, J. A., Karaczyn, A., Adams, T. & Verdi, J. M. A role for NRAGE in NF-κB activation through the non-canonical BMP pathway. *BMC Biol.* **8,** 7 (2010).
31. Lien, W. H., Gelfand, V. I. & Vasioukhin, V. α-E-catenin binds to dynamitin and regulates dynactin-mediated intracellular traffic. *J. Cell Biol.* **183,** 989–997 (2008).
32. Pickart, C. M. & Fushman, D. Polyubiquitin chains: polymeric protein signals. *Curr. Opin. Chem. Biol.* **8,** 610–616 (2004).
33. Bren, G. D. *et al.* Transcription of the RelB gene is regulated by NF-κB. *Oncogene* **20,** 7722–7733 (2001).
34. Gyorffy, B. *et al.* An online survival analysis tool to rapidly assess the effect of 22,277 genes on breast cancer prognosis using microarray data of 1,809 patients. *Breast Cancer Res. Treat.* **123,** 725–731 (2010).
35. Ding, L. *et al.* Genome remodelling in a basal-like breast cancer metastasis and xenograft. *Nature* **464,** 999–1005 (2010).
36. Kobielak, A. & Fuchs, E. Links between α-catenin, NF-κB, and squamous cell carcinoma in skin. *Proc. Natl Acad. Sci. USA* **103,** 2322–2327 (2006).
37. Hu, Y. *et al.* Abnormal morphogenesis but intact IKK activation in mice lacking the IKKα subunit of IκB kinase. *Science* **284,** 316–320 (1999).
38. Yan, J. *et al.* Inactivation of BAD by IKK inhibits TNFα-induced apoptosis independently of NF-κB activation. *Cell* **152,** 304–315 (2013).
39. Ben-Neriah, Y. & Karin, M. Inflammation meets cancer, with NF-κB as the matchmaker. *Nat. Immunol.* **12,** 715–723 (2011).
40. Gilmore, T. D. Introduction to NF-κB: players, pathways, perspectives. *Oncogene* **25,** 6680–6684 (2006).
41. Karin, M., Cao, Y., Greten, F. R. & Li, Z. W. NF-κB in cancer: from innocent bystander to major culprit. *Nat. Rev. Cancer* **2,** 301–310 (2002).
42. Pianetti, S., Arsura, M., Romieu-Mourez, R., Coffey, R. J. & Sonenshein, G. E. Her-2/neu overexpression induces NF-κB via a PI3-kinase/Akt pathway involving calpain-mediated degradation of IκB-α that can be inhibited by the tumor suppressor PTEN. *Oncogene* **20,** 1287–1299 (2001).

METHODS

Cell culture. The HMLE immortalized human mammary epithelial cells were described previously[43]. The SUM159 cell line, provided by S. Ethier, was cultured as described (http://www.asterand.com/asterand/human_tissues/159PT.htm). Cell lines MCF10A, MCF7, T47D, BT549, MDA-MB-231, MDA-MB-157, MDA-MB-436, MDA-MB-468 and HEK293T were purchased from the American Type Culture Collection and cultured under conditions specified by the provider.

RNA isolation and qPCR with reverse transcription. Total RNA was isolated using the RNeasy Mini Kit (Qiagen) and was then reverse transcribed with an iScript cDNA Synthesis Kit (Bio-Rad). The resulting complementary DNA was analysed by qPCR using the SYBR Green Gene Expression Assays (Bio-Rad), and data were normalized to an endogenous control, GAPDH. Real-time PCR and data collection were performed on a CFX96 instrument (Bio-Rad). The primers used in this study are listed in Supplementary Table 2.

Plasmids and shRNA. The following shRNA and ORF clones were obtained from Open Biosystems through the shRNA and ORFeome Core facility of The University of Texas MD Anderson Cancer Center: human *CTNNA1* shRNA, V3LMM-492867 (5′-AATTTGTAGACATCTGCCA-3′, designated CTNNA1 shRNA1) and V3LMM-492872 (5′-TGCTTGTTCAACAGATGCA-3′, designated CTNNA1 shRNA3); human IκBα shRNA, V3LHS_375160 (5′-CGTCCTCTGTGAACTCCGT-3′, designated IκBα shRNA3) and V3LHS_410688 (5′-TTTTTGATAACCTTCTCCA-3′, designated IκBα shRNA5); human RelA shRNA, V3LHS_633762 (5′-ATCTGTGCTCCTCTCGCCT-3′, designated RelA shRNA4) and V3LHS_633764 (5′-TCTATAGGAACTTGGAAGG-3′, designated RelA shRNA5); human α-catenin ORF, PLOH-10000388. The human IκBα ORF was cloned from the cDNA of HMLE cells. The α-catenin and IκBα ORFs were subcloned into an SFB (S-protein, FLAG tag and streptavidin-binding peptide)-tagged expression vector (provided by J. Chen). The pNFκB luciferase reporter construct was purchased from Stratagene (219078-51). The vectors used in this study are listed in Supplementary Table 3.

Human cancer pathway PCR array analysis. The Cancer PathwayFinder RT^2 Profiler PCR Array, consisting of 84 genes representative of 6 tumour signalling pathways, was used to profile α-catenin-expressing MDA-MB-157 cells according to the manufacturer's instructions (http://www.sabiosciences.com/rt_pcr_product/HTML/PAHS-033A.html). Briefly, total RNA was extracted and reverse transcribed into cDNA using an RT^2 First Strand Kit (Qiagen). The cDNA was combined with an RT^2 SYBR Green qPCR Master Mix (Qiagen), and then equal aliquots of this mixture (25 μl) were added to each well of the same PCR Array plate that contained the predispensed gene-specific primer sets. Real-time PCR and data collection were performed on a CFX96 instrument (Bio-Rad).

Lentiviral transduction. Lentivirus was produced and target cells were infected as described previously[44]. Virus-containing supernatant was collected 48 and 72 h after co-transfection of pCMV-VSV-G, pCMVΔ8.2 and the shRNA- or ORF-containing vector into HEK293T cells, and then added to the target cells. Twenty-four hours later, the infected cells were selected with 10 μg ml^{-1} blasticidin (for pLOC vector) or 2 μg ml^{-1} puromycin (for pGIPZ vector).

Enzyme-linked immunosorbent assay. Cells were grown to near confluence in serum-containing medium, washed three times with PBS and then incubated with serum-free medium (DMEM/F12 containing penicillin and streptomycin). After a 48-h (for IL-8) or 96-h (for TNF-α) incubation, conditioned medium was collected for enzyme-linked immunosorbent assay using the Quantikine Kit (IL8: D8000C; TNF-α: DTA00C, R&D Systems) according to the manufacturer's protocol.

Cell proliferation assay. To determine growth curves, we plated equal numbers of cells in 12-well plates in triplicate. Beginning on day 3, cells were fixed with 10% methanol and stained with 0.1% crystal violet (dissolved in 10% methanol) every day. After staining, wells were washed three times with PBS and destained with acetic acid, and the absorbance of the crystal violet solution was measured at 590 nm.

Anchorage-independent growth assay. Cells were suspended in 1 ml of 0.35% low-melting-point agarose (Invitrogen) in DMEM supplemented with 10% FBS and plated in triplicate in 6-well plates on 1 ml of presolidified 0.65% agarose in the same medium, with 1 ml of medium covering the cells. After incubation at 37 °C in 5% CO_2 for 3–6 weeks, plates were stained with crystal violet and scanned on a GelCount system (Oxford Optronix). Colonies were counted by using the ImageJ program (http://rsbweb.nih.gov/ij/download.html).

Transwell migration assay. Cells ($1–2 \times 10^5$) were plated in the top chamber with the non-coated membrane (24-well insert; pore size, 8 μm; BD Biosciences) in medium without serum or growth factors. Medium supplemented with growth factors (for MCF10A) or serum (for BT549) was used as a chemoattractant in the lower chamber. The cells were incubated for 20 h, and cells that did not migrate through the pores were removed with a cotton swab. Cells on the lower surface of the membrane were stained with the Diff-Quick Staining Set (Dade) and counted.

Luciferase reporter assay. Cells of 70% confluence in 6-well plates were transfected using X-tremeGene9 (Roche). The firefly luciferase reporter gene construct (0.5 μg) and the pRL-SV40 *Renilla* luciferase construct (10 ng, for normalization) were used for co-transfection. Cell extracts were prepared 24–48 h after transfection, and the luciferase activity was measured using the Dual-Luciferase Reporter Assay System (Promega).

Immunoblotting. Western blot analyses were performed with precast gradient gels (Bio-Rad) using standard methods. Briefly, cells were lysed in radioimmunoprecipitation assay (RIPA) buffer containing protease inhibitors (Roche) and phosphatase inhibitors (Sigma). Proteins were separated by sodium dodecyl sulphate–polyacrylamide gel electrophoresis (SDS–PAGE) and blotted onto a PVDF membrane (Bio-Rad). Membranes were probed with the specific primary antibodies and then with peroxidase-conjugated secondary antibodies. The bands were visualized by chemiluminescence (Denville Scientific). The following antibodies were used: antibodies against α-catenin (1:1,000, Sigma, SAB1402163; 1:1,000, Cell Signaling Technology, 3240, Clone 23B2), α-tubulin (1:3,000, Sigma, T5168, Clone B-5-1-2), β-catenin (1:2,000, BD Transduction Laboratories, 610154, Clone 14/Beta-catenin), E-cadherin (1:1,000, BD Transduction Laboratories, 610182, Clone 36/E-cadherin), p-RelA (Ser 536; 1:1,000, Cell Signaling Technology, 3033, Clone 93H1), RelA (1:1,000, Cell Signaling Technology, 6956; 1:1,000, Cell Signaling Technology, 8242, Clone L8F6), RelB (1:1,000, Cell Signaling Technology, 4922, Clone C1E4), p-IκBα (Ser 32/36; 1:1,000, Cell Signaling Technology, 9246, Clone 5A5), IκBα (1:1,000, Cell Signaling Technology, 9242), IKKβ (1:1,000, Cell Signaling Technology, 2678, Clone 2C8), p-IKKα/β (Ser 176/180; 1:1,000, Cell Signaling Technology, 2697, Clone 16A6), FLAG (1:2,000, Sigma, F3165; 1:2,000, Sigma, F7425, Clone M2), lamin A (1:2,000, Abcam, ab8980, Clone 133A2), 20S proteasome subunit α4 (1:1,000, Enzo Life Sciences, PW8120, Clone MCP34), HA (1:1,000, Roche, 11583816001, Clone 12CA5), MYC (1:2,000, Cell Signaling Technology, 2276, Clone# 9B11), YAP (1:1,000, Cell Signaling Technology, 4912), p-YAP (1:1,000, Cell Signaling Technology, 4911), β-actin (1:5,000, Sigma, A5441, Clone AC-15) and HSP90 (1:2,000 BD Transduction Laboratories, 610419, Clone 68/Hsp90). The ImageJ program (http://rsbweb.nih.gov/ij/download.html) was used for densitometric analysis of western blots, and the quantification results were normalized to the loading control.

Cytoplasmic and nuclear fractionation. Nuclear and cytoplasmic proteins were fractionated using the NE-PER Nuclear and Cytoplasmic Extraction Kit (Thermo) according to the manufacturer's protocol. After fractionation, 30 μg of protein was used for western blot analysis of α-catenin, RelA, RelB and IκBα in the cytoplasm and nucleus. α-tubulin and lamin A were used as cytoplasmic and nuclear markers, respectively.

Co-immunoprecipitation and pulldown assays. Co-immunoprecipitation was performed as described previously[45]. Cells were lysed in E1A lysis buffer (250 mM NaCl, 50 mM HEPES (pH 7.5), 0.1% NP-40, 5 mM EDTA and protease inhibitor cocktail (Sigma)). The antibodies against α-catenin (1:500, Sigma, C2081) and IκBα (1:500, Cell Signaling Technology, 9242) were used for immunoprecipitation. The SFB pulldown experiment was done as described previously[46]. Briefly, HEK293T cells were transfected with SFB-tagged protein and lysed in NETN buffer (200 mM Tris-HCl (pH 8.0) 100 mM NaCl, 0.05% NP-40, 1 mM EDTA and protease inhibitor cocktail (Sigma)) for 20 min at 4 °C. Crude lysates were subjected to centrifugation at 12,000*g* for 15 min at 4 °C. Supernatants were incubated with S-protein beads for 4 h (Novagen). The beads were washed three times with NETN buffer. Proteins were eluted by boiling in 1× SDS running buffer and subjected to SDS–PAGE for immunoblotting.

ChIP assay. Cells were grown to 80% confluence, and crosslinking was performed with 1% formaldehyde for 10 min. ChIP assays were performed using a Magna ChIP G Chromatin Immunoprecipitation Kit (Millipore) according to the manufacturer's instructions. After immunoprecipitation with an antibody against RelA (Cell Signaling Technology, 8242) or normal rabbit IgG, protein–DNA crosslinks were reversed. DNA was then purified to remove the chromatin proteins and analysed by qPCR using the Qiagen EpiTect ChIP qPCR Primers (catalogue number GPH1006956(-)01A).

***In vivo* tumorigenesis study.** All animal experiments were performed in accordance with a protocol approved by the Institutional Animal Care and Use Committee of MD Anderson Cancer Center. When used in a power calculation,

DOI: 10.1038/ncb2909

our sample size predetermination experiments indicate that 5 mice per group can identify the expected effect of α-catenin on tumour size and weight ($P < 0.05$) with 100% power. Animals were randomly assigned to different groups. Six- to eight-week-old female nude mice were used for subcutaneous injection of human breast cancer cells. Tumour cells in 30 μl of growth medium (mixed with Matrigel at a 1:1 ratio) were injected subcutaneously using a 100-μl Hamilton Microliter syringe. Tumour size was measured once a week using a caliper, and tumour volume was calculated using the standard formula $0.5 \times L \times W^2$, where L is the longest diameter and W is the shortest diameter. Mice were euthanized when they met the institutional euthanasia criteria for tumour size and overall health condition. The tumours were removed, photographed and weighed. The freshly dissected tumour tissues were fixed in 10% buffered formalin overnight, washed with PBS, transferred to 70% ethanol, embedded in paraffin, sectioned and stained with haematoxylin and eosin. A laboratory technician (M.W.) who provided animal care and measured tumour growth was blinded to the group allocation during all animal experiments and outcome assessment.

Immunohistochemistry. Samples were deparaffinized and rehydrated. Antigen was retrieved using 0.01 M sodium-citrate buffer (pH 6.0) at a sub-boiling temperature for 10 min after boiling in a microwave oven. To block endogenous peroxidase activity, the sections were incubated with 3% hydrogen peroxide for 10 min. After 1 h of pre-incubation in 5% normal goat serum to prevent nonspecific staining, the samples were incubated with the antibody against IκBα (1:50, Cell Signaling Technology, 4814) or TNF-α (1:50, Novus Biologicals, NBP1-19532) at 4 °C overnight. The sections were incubated with a biotinylated secondary antibody (1:500, biotinylated anti-rabbit IgG(H+L), Vector Laboratories, BA-1000 for TNF-α; 1:500, biotinylated anti-mouse IgG(H+L), Vector Laboratories, BA-9200 for IκBα) and then incubated with an avidin–biotin peroxidase complex solution (Vector Laboratories, PK-6100) for 30 min at room temperature. Colour was developed using the DAB (diaminobenzidine) Substrate Kit (BD Biosciences, 550880). Counterstaining was carried out using Harris modified haematoxylin.

TCGA data analysis. We obtained level 3 data for mRNA expression and gene methylation of human breast tumours from Synapse (http://synapse.org; syn1461151). mRNA expression was measured using the Agilent 244K Custom Gene Expression G4502A-07-3 (microarray) or the Illumina HiSeq 2000 RNA Sequencing version 2 analysis platform (RNA-Seq by Expectation Maximization, RSEM). Methylation was measured by using the Illumina Infinium Human DNA Methylation 450 platform. The breast cancer subtype information (luminal A, luminal B, basal-like and HER2 subtypes) was described previously[10]. The expression levels of *CTNNA1* in normal and cancer samples for each subtype were compared using the Wilcoxon test. The association between *CTNNA1* expression level and its gene methylation was assessed by the Spearman rank correlation test.

Statistical analysis. Each experiment was repeated three times or more. Unless otherwise noted, data are presented as mean ± s.e.m., and Student's t-test (unpaired, two-tailed) was used to compare two groups of independent samples. The data analysed by t-test meet normal distribution; we used an F-test to compare variances, and the variances are not significantly different. Therefore, when using an unpaired t-test, we assumed equal variance, and no samples were excluded from the analysis. The log-rank test was used to compare Kaplan–Meier survival curves. Statistical methods used for TCGA data analysis are described above. $P < 0.05$ was considered statistically significant.

Accession number. The accession number of TCGA breast cancer data is syn1461151 (https://www.synapse.org/{#}!Synapse:syn1461151)

43. Elenbaas, B. *et al.* Human breast cancer cells generated by oncogenic transformation of primary mammary epithelial cells. *Genes Dev.* **15,** 50–65 (2001).
44. Stewart, S. A. *et al.* Lentivirus-delivered stable gene silencing by RNAi in primary cells. *RNA* **9,** 493–501 (2003).
45. Yang, W. L. *et al.* The E3 ligase TRAF6 regulates Akt ubiquitination and activation. *Science* **325,** 1134–1138 (2009).
46. Wang, W. *et al.* PTPN14 is required for the density-dependent control of YAP1. *Genes Dev.* **26,** 1959–1971 (2012).

DOI: 10.1038/ncb2909

nature cell biology

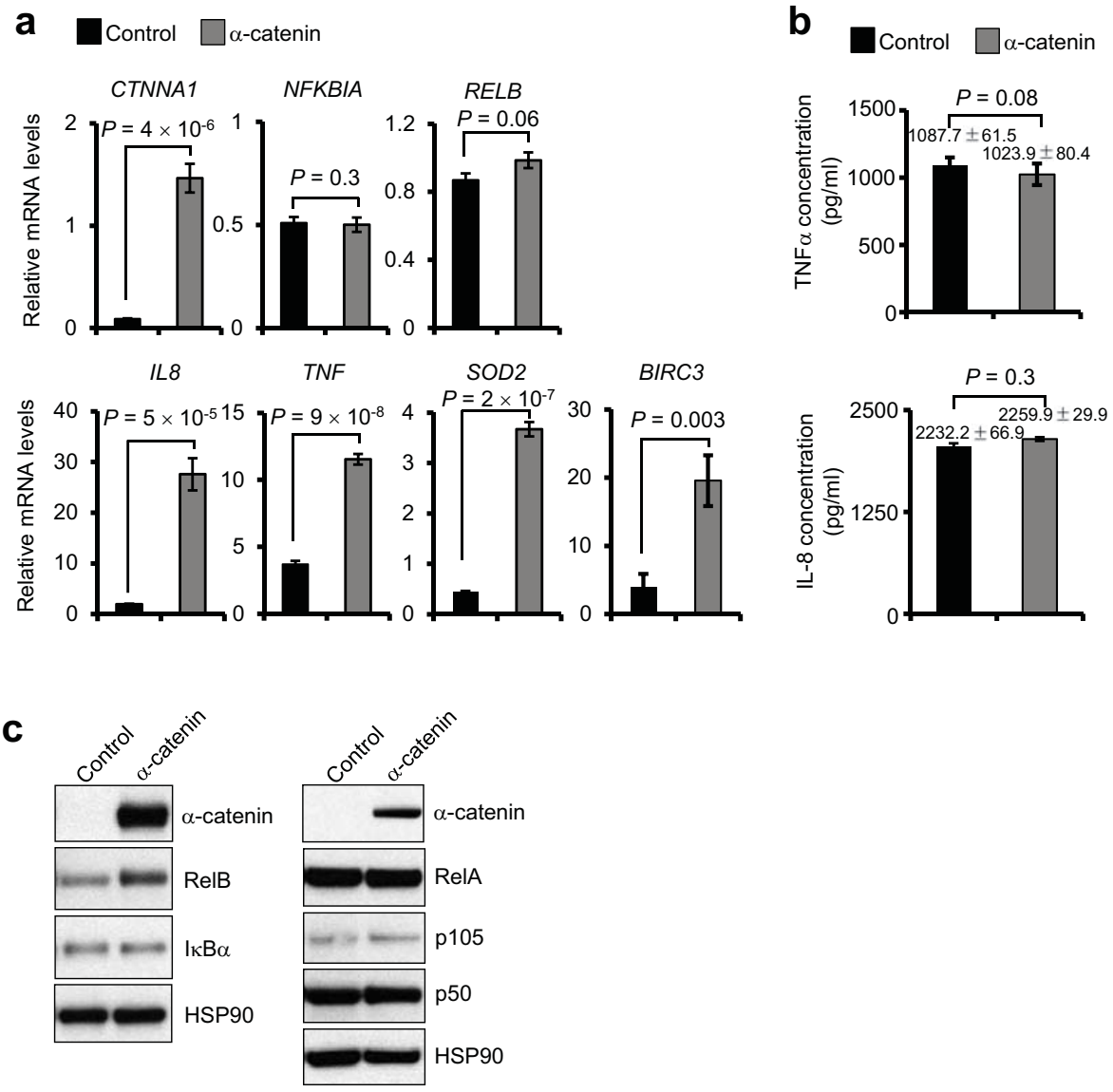

Supplementary Figure 1 α-catenin does not inhibit NF-κB signaling in E-cadherin-positive breast cancer cells. (**a**) qPCR of *CTNNA1*, *NFKBIA*, *RELB*, *IL8*, *TNF*, *SOD2* and *BIRC3* in α-catenin-transduced MDA-MB-468 cells. $n = 3$ samples per group. (**b**) ELISA of TNFα and IL-8 secreted by α-catenin-transduced MDA-MB-468 cells. $n = 3$ wells per group. (**c**) Immunoblotting of α-catenin, RelB, IκBα, RelA, p105, p50 and HSP90 in α-catenin-transduced MDA-MB-468 cells. Data in (**a**) and (**b**) are the mean of biological replicates from a representative experiment, and error bars indicate s.e.m. Statistical significance was determined by a two-tailed, unpaired Student's *t*-test. The experiments were repeated three times. The source data can be found in Supplementary Table 4. Uncropped images of blots are shown in Supplementary Fig. 7.

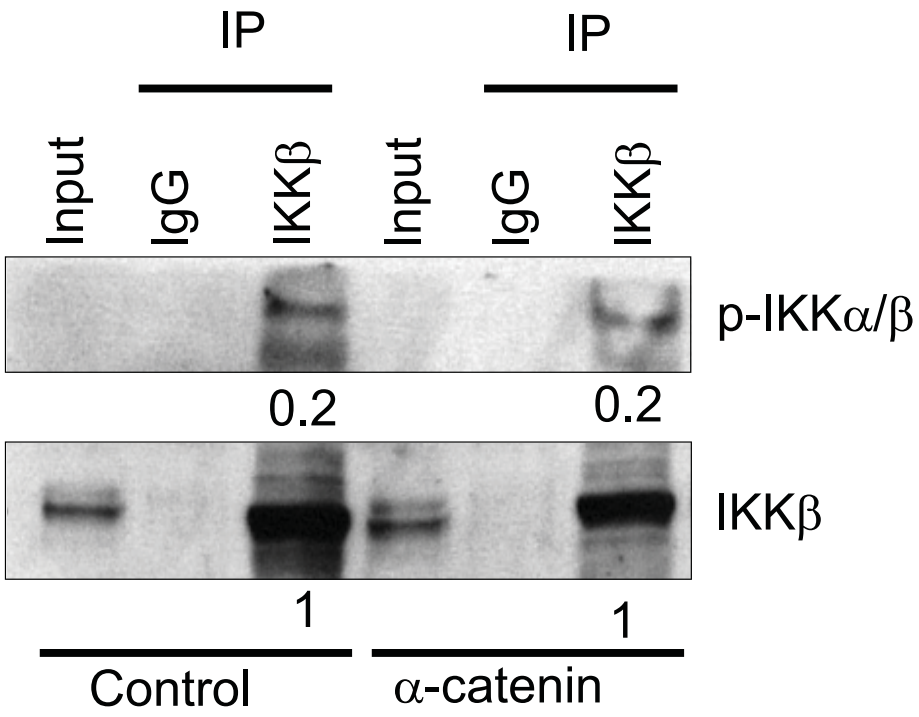

Supplementary Figure 2 α-catenin does not regulate IKK phosphorylation in MDA-MB-157 cells. Endogenous IKKβ was immunoprecipitated from mock-infected or α-catenin-transduced MDA-MB157 cells and immunoblotted with antibodies to p-IKK and IKKβ. Cells were treated with TNFα (20 ng/ml). Uncropped images of blots are shown in Supplementary Fig. 7.

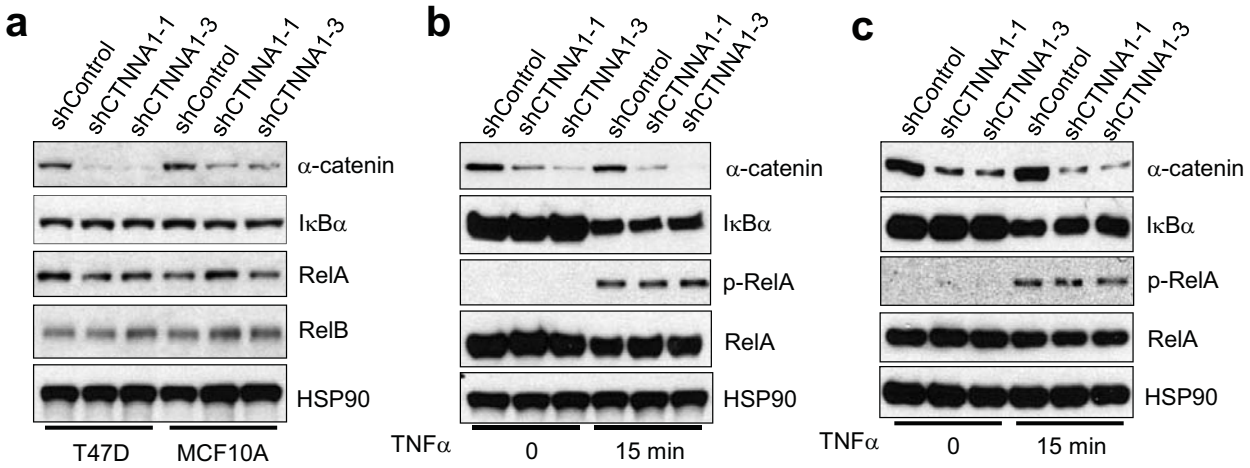

Supplementary Figure 3 α-catenin does not regulate IκBα, RelA and RelB protein levels in luminal-like mammary cells. (**a**) Immunoblotting of α-catenin, IκBα, RelA, RelB and HSP90 in T47D and MCF10A cells transduced with two independent α-catenin shRNAs. (**b, c**) Immunoblotting of α-catenin, IκBα, p-RelA, RelA and HSP90 in α-catenin shRNA-transduced T47D (**b**) and MCF10A (**c**) cells, with or without TNFα treatment (20 ng/ml). Uncropped images of blots are shown in Supplementary Fig. 7.

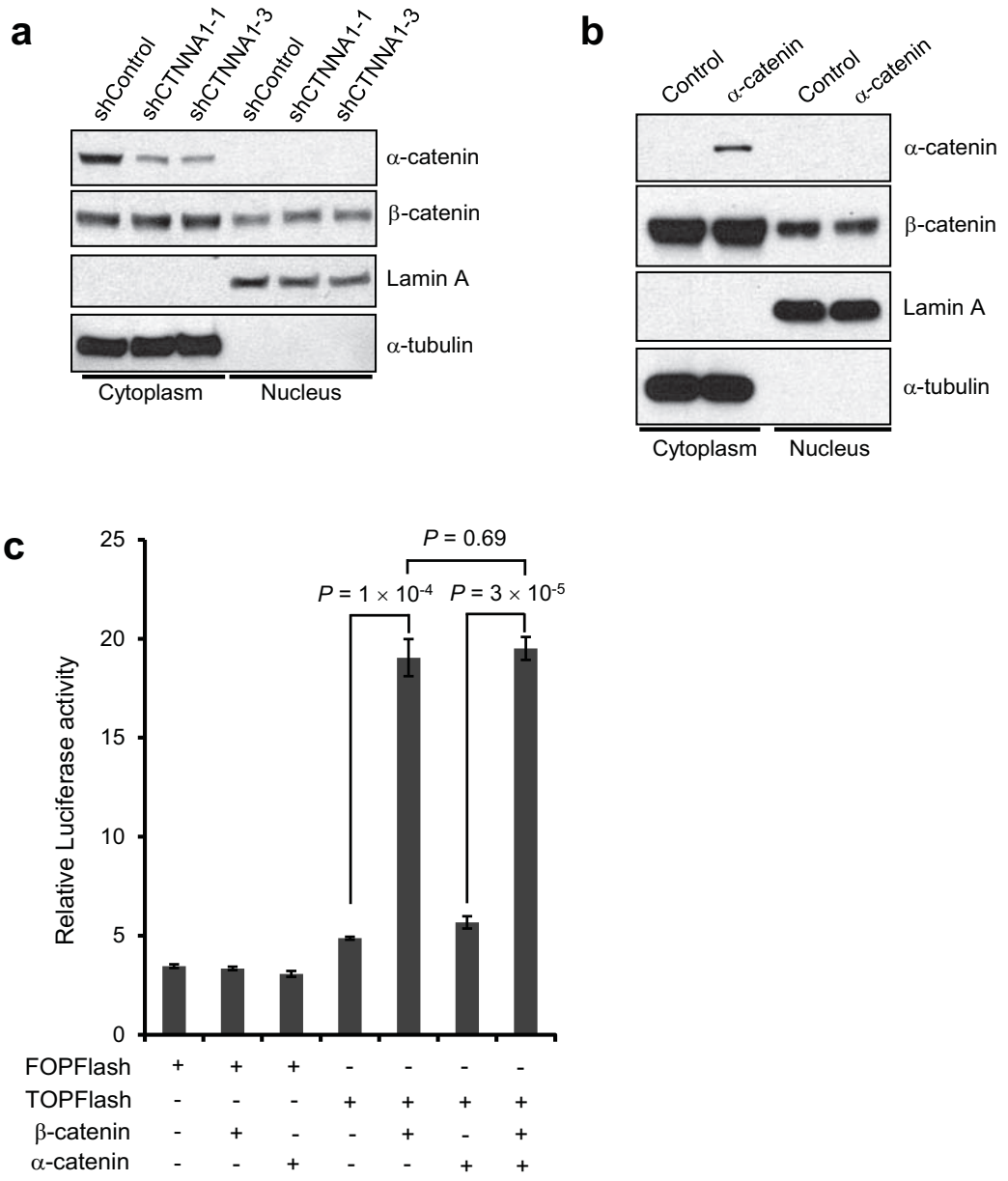

Supplementary Figure 4 α-catenin does not modulate β-catenin in basal-like breast cancer cells. (**a**) Immunoblotting of α-catenin and β-catenin in cytoplasmic and nuclear fractions of BT549 cells transduced with two independent α-catenin shRNAs. (**b**) Immunoblotting of α-catenin and β-catenin in cytoplasmic and nuclear fractions of α-catenin-transduced MDA-MB-157 cells. α-tubulin and lamin A were used as cytoplasmic and nuclear markers, respectively, in (**a**) and (**b**). (**c**) Luciferase assays of β-catenin activity in MDA-MB-157 cells transfected with the Fopflash or Topflash luciferase reporter alone or in combination with α-catenin or β-catenin, or both. The Topflash construct contains multiple TCF/LEF-binding sites in the promoter of a firefly luciferase reporter gene and the derived Fopflash construct contains mutated TCF/LEF binding sites. n = 3 wells per group. Data in (**c**) are the mean of biological replicates from a representative experiment, and error bars indicate s.e.m. Statistical significance was determined by a two-tailed, unpaired Student's t-test. The experiments were repeated three times. The source data can be found in Supplementary Table 4. Uncropped images of blots are shown in Supplementary Fig. 7.

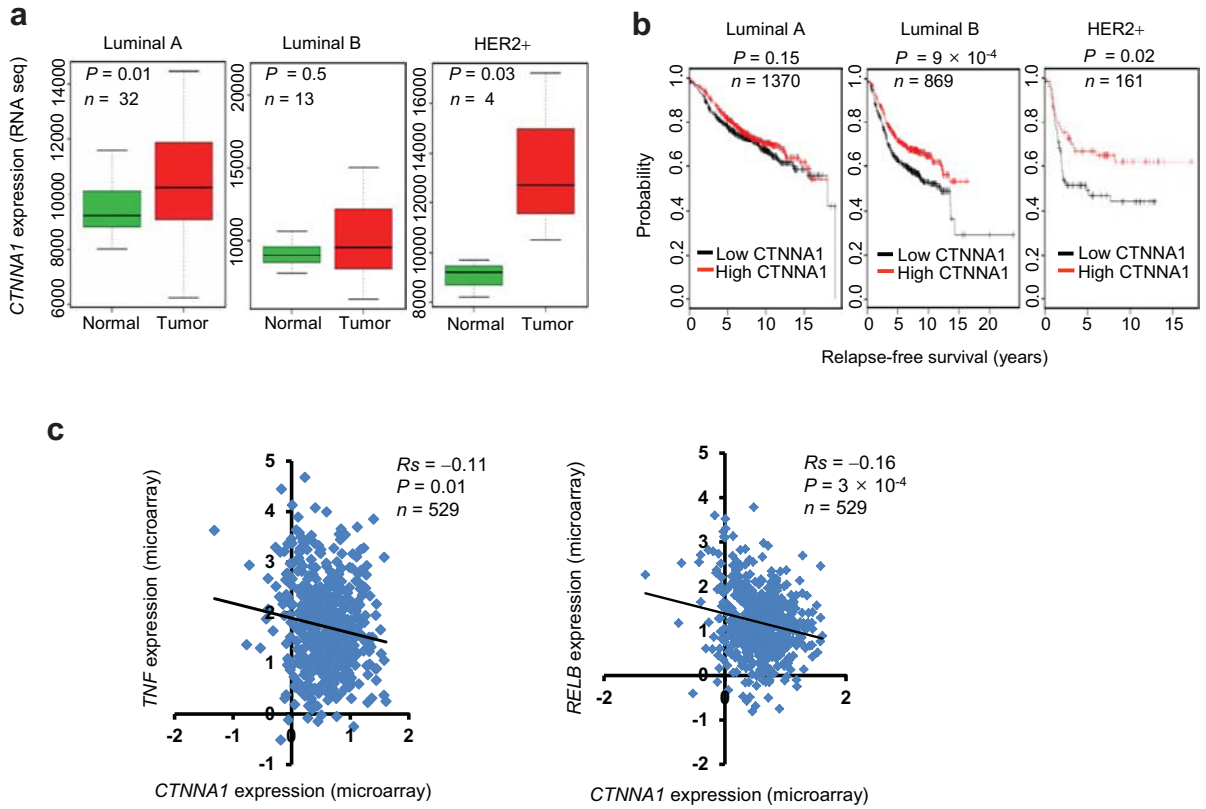

Supplementary Figure 5 α-catenin negatively correlates with NF-κB signaling components in human breast tumors. (**a**) Box plots comparing *CTNNA1* expression in normal breast tissues and in luminal A, luminal B and HER2+ breast tumors ($n = 32$, 13 and 4 patient samples, respectively). Statistical significance was determined by the Wilcoxon test. The boxes show the median and the interquartile range. The whiskers show the minimum and maximum. (**b**) Kaplan-Meier curves of relapse-free survival times of total breast cancer patients and patients with luminal A, luminal B or HER2+ breast cancer ($n = 1370$, 869 and 161 patient samples, respectively), stratified by *CTNNA1* expression levels. Statistical significance was determined by the log-rank test. (**c**) Scatterplots showing the inverse correlation of *CTNNA1* with *TNF* (left panel) or *RELB* (right panel) expression in human breast tumors, based on the microarray data from TCGA. Statistical significance was determined by Spearman rank correlation test. *Rs* = Spearman rank correlation coefficient.

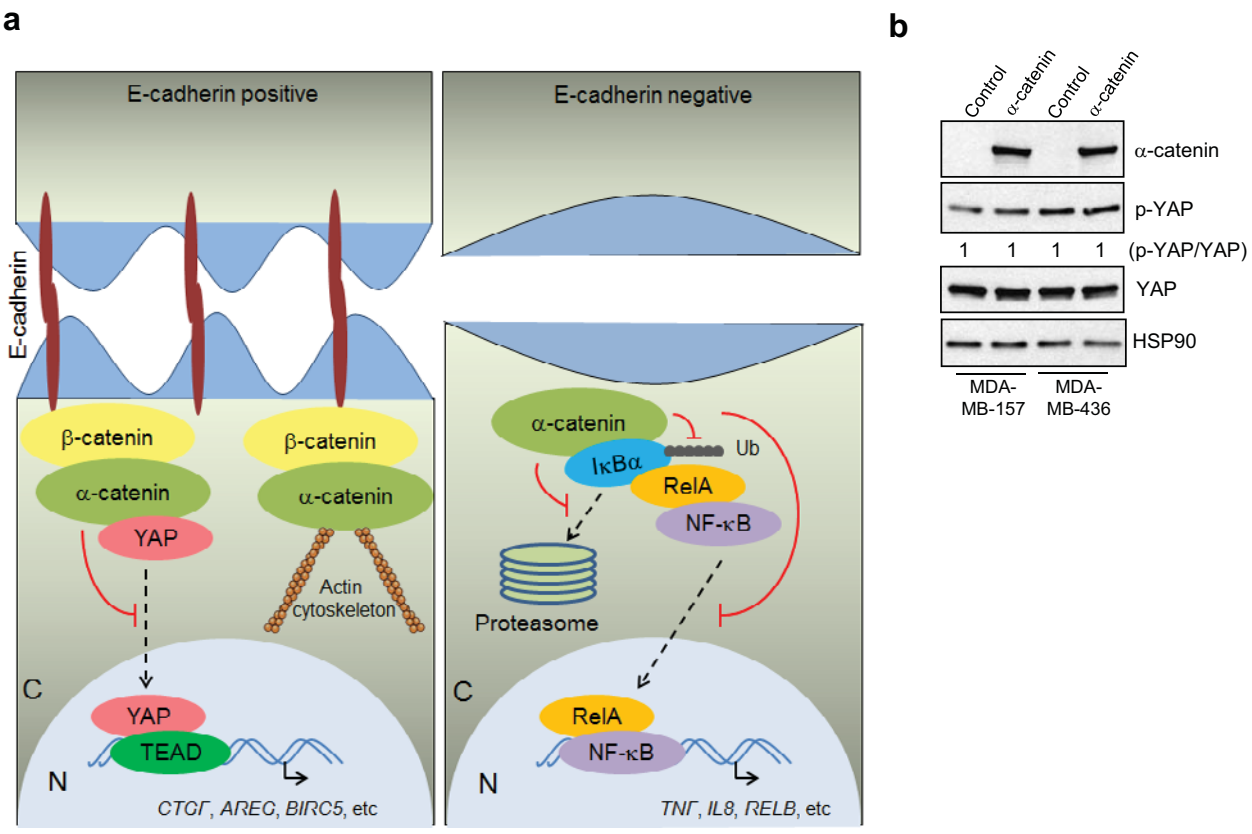

Supplementary Figure 6 α-catenin mechanisms of action. (**a**) Cytoplasmic α-catenin and α-catenin localized to the cadherin-catenin complex regulate different pathways through different mechanisms. C: cytoplasm; N: nucleus; Ub: ubiquitin chain. (**b**) Immunoblotting of α-catenin, p-YAP, YAP and HSP90 in mock-infected and α-catenin-transduced MDA-MB-157 and MDA-MB-436 cells. Uncropped images of blots are shown in Supplementary Fig. 7.

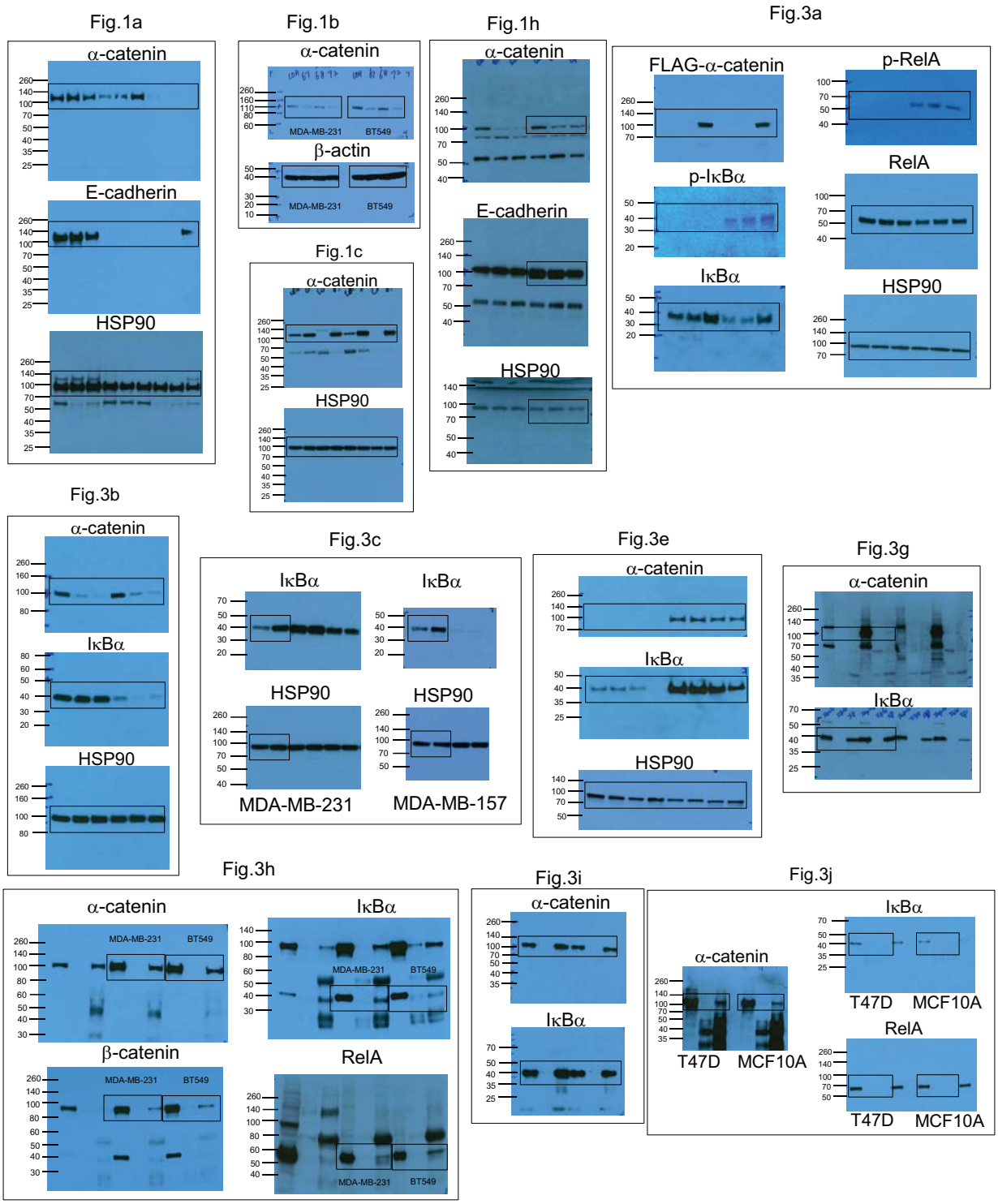

Supplementary Figure 7 Uncropped images of immunoblots.

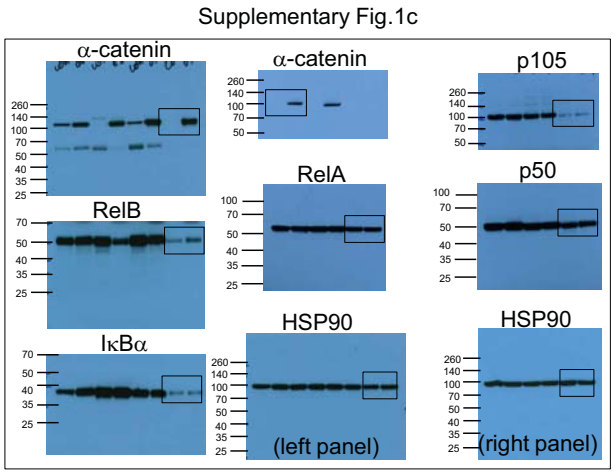

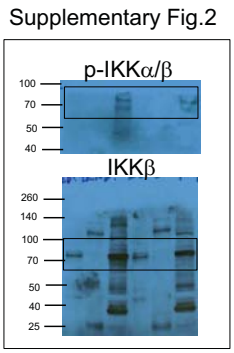

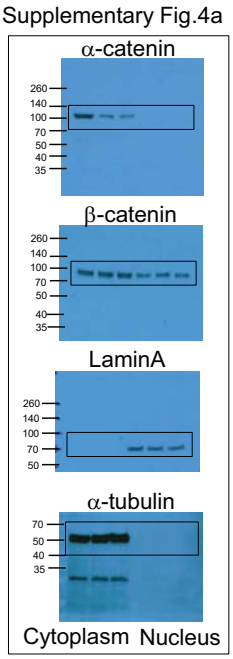

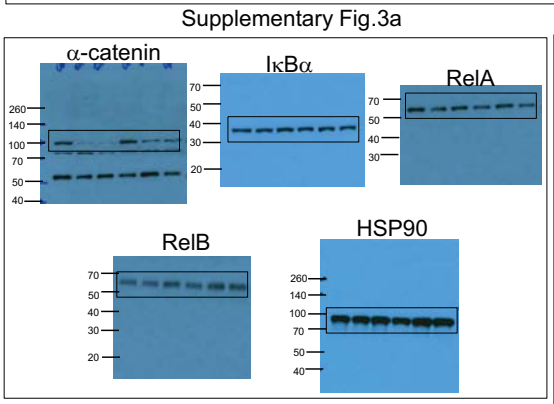

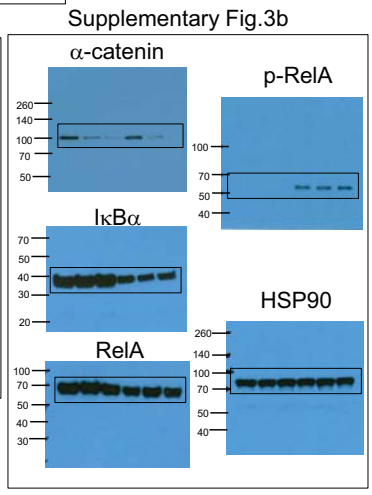

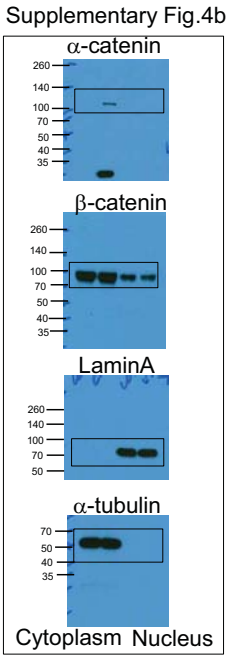

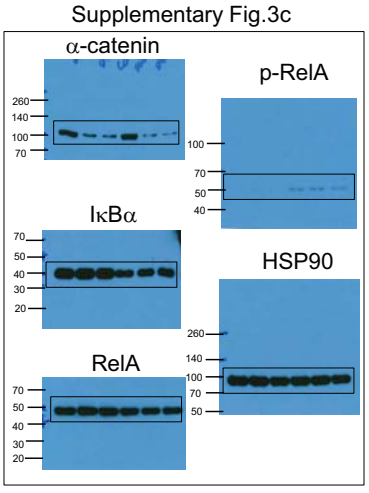

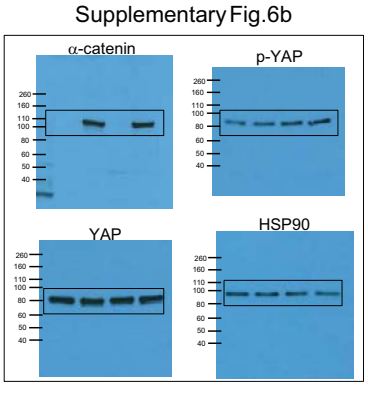

Supplementary Figure 7 continued